

UNIVERSITY OF WOLLONGONG

DOCTORAL THESIS

Thesis Title

Author:
Jesse GREENSLADE

Supervisor:
Dr. Jenny FISHER

*A thesis submitted in fulfillment of the requirements
for the degree of Doctor of Philosophy
in the*

Centre of Atmospheric Chemistry
Chemistry Department

January 30, 2018

Declaration of Authorship

I, Jesse GREENSLADE, declare that this thesis titled, “Thesis Title” and the work presented in it are my own. I confirm that:

- This work was done wholly or mainly while in candidature for a research degree at this University.
- Where any part of this thesis has previously been submitted for a degree or any other qualification at this University or any other institution, this has been clearly stated.
- Where I have consulted the published work of others, this is always clearly attributed.
- Where I have quoted from the work of others, the source is always given. With the exception of such quotations, this thesis is entirely my own work.
- I have acknowledged all main sources of help.
- Where the thesis is based on work done by myself jointly with others, I have made clear exactly what was done by others and what I have contributed myself.

Signed:

Date:

"Thanks to my solid academic training, today I can write hundreds of words on virtually any topic without possessing a shred of information, which is how I got a good job in journalism."

Dave Barry

Contents

Declaration of Authorship	iii
Abstract	vii
Acknowledgements	ix
1 Introduction and Literature Review	1
1.1 The atmosphere	1
1.1.1 Structure	1
1.1.2 Chemistry	1
Hydroxyl radicals	1
Nitrate radicals	2
1.2 Ozone	2
1.2.1 Stratosphere to troposphere transport	4
1.2.2 Chemical production	5
1.3 VOCs	5
1.3.1 Isoprene	7
1.3.2 Emissions	8
1.3.3 The isoprene cascade	9
Oxidation	9
Ozonolysis	11
SOA	11
Night time chemistry	12
1.4 HCHO	14
1.4.1 Sources and sinks	15
1.4.2 Measurement techniques	16
DOAS	16
Satellite measurements	19
OMI	20
AMF	22
Uncertainties	22
1.4.3 Glyoxyl TODO: move somewhere fitting?	24
1.5 Modelling	25
1.5.1 Chemistry	25
GEOS-Chem	27
Box models	27
1.5.2 Emissions	28
MEGAN	28
1.5.3 Satellite inversion	30

1.5.4	Uncertainties?	33
	Emissions Inventories	33
	Resolution	34
	Chemistry mechanisms	34
	Clouds	35
	Soil Moisture	35
1.6	Australia	36
1.6.1	VOCs	36
1.6.2	Air quality	38
1.6.3	Measurements	38
1.7	Aims	38
1.8	Data Access	39
2	Modelling and Data	41
2.1	List of runs and outputs used in my work TODO: good place for this?	41
2.1.1	GEOS-Chem	41
2.1.2	CAABA/MECCA	42
2.1.3	Reading Data	42
	CAABA/MECCA outputs	42
	GEOS-Chem Satellite output	42
	HEMCO diagnostics	42
2.2	GEOS-Chem	42
2.2.1	GEOS-Chem isoprene modelling	42
	Outline	42
	Emissions from MEGAN	44
2.2.2	Chemical Mechanisms	44
2.2.3	Running GEOS-Chem (before isop?)	45
	Installation and requirements	45
	Options	45
	Tropospheric chemistry run	45
	UCX run	45
2.2.4	Run comparisons	45
2.3	CAABA/MECCA	49
2.4	Campaigns and datasets	49
2.4.1	OMI Satellite measurements	49
	OMI HCHO	49
	OMI NO ₂	49
	Marine and Urban MBA ? (MUMBA)	50
	Sydney Particle Studies (SPS1, SPS2)	50
2.5	Analysing output	50
2.5.1	Circadian emissions cycle	50
2.5.2	HCHO: Simulated vs Measured	50
2.5.3	Accounting for Fires	51
2.5.4	Accounting for NO _x	51
2.5.5	HCHO Comparisons	51

3	Stratospheric ozone intrusions	57
3.1	Introduction	57
3.2	Data and Methods	59
3.2.1	Ozonesonde record in the Southern Ocean	59
3.2.2	Model description	61
3.2.3	Characterisation of STT events and associated fluxes	63
3.2.4	Biomass burning influence	65
3.2.5	Classifying synoptic conditions during STT events	65
3.3	STT event climatologies	66
3.4	Simulated ozone columns	69
3.5	Stratosphere-to-troposphere ozone flux from STT events	71
3.5.1	Method	71
3.5.2	Results	76
3.5.3	Comparison to literature	76
3.6	Sensitivities and limitations	81
3.6.1	Event detection	81
3.6.2	Flux calculations	82
3.7	Conclusions	83
3.8	Contributions and Acknowledgements	84
4	Biogenic Isoprene emissions in Australia	85
4.1	Outline TODO: move into intro?	85
4.2	Introduction	85
4.3	Data	87
4.3.1	OMI NO ₂	87
4.3.2	OMI HCHO	87
4.3.3	Drought Index	87
4.3.4	GEOS-Chem output	87
4.4	Modelling	87
4.4.1	GEOS-Chem simulation	87
4.4.2	CAABA/MECCA simulations	88
4.5	Methods	88
4.5.1	CAABA/MECCA Box model: isoprene source classifications	88
4.5.2	Recalculation of OMI HCHO	89
4.5.3	Calculation of Emissions	90
4.5.4	Emissions drivers	92
4.5.5	HCHO Products and yield	92
4.5.6	Accounting for smearing	95
4.6	Results	98
4.6.1	Emissions affect on GEOS-Chem	98
4.6.2	Emissions comparisons	98
4.7	Uncertainty	98
4.7.1	Model Uncertainty	99
4.7.2	Satellite Uncertainty	99

5	TODO: move to biogenic isop chapter: Formaldehyde product over Australia	101
5.1	Australian Biogenic Volatile Organic Compounds (BVOCs)	101
5.1.1	Isoprene, Monoterpenes	101
5.1.2	Biomass Burning	102
5.1.3	MEGAN	102
5.2	Satellite HCHO measurements	102
5.2.1	Satellite Retrievals	102
5.2.2	OMI Algorithm BOAS	103
5.2.3	Optical Depth (τ)	104
5.2.4	Scattering	105
5.2.5	Absorption cross section and number density	105
5.2.6	Air Mass Factors	105
5.2.7	OMI HCHO data products	106
5.2.8	HCHO Vertical Column Calculation	106
5.2.9	Uncertainty in OMI total columns (Moved)	109
5.2.10	Reference sector correction for comparison of products to various models	109
5.3	Recalculating HCHO from satellite(OMI) data over Australia	110
5.3.1	Process Outline	110
5.3.2	Quality filtering OMI HCHO slant columns	111
5.3.3	Reading OMHCHO daily slant columns	113
5.3.4	Regridding to 0.25 by 0.3125 8-day averaged vertical columns	113
5.3.5	Filtering pyrogenic HCHO	114
5.3.6	Filtering anthropogenic HCHO	116
5.3.7	Recalculating the AMF to create our own vertical HCHO columns	116
5.3.8	AMF code from Paul Palmer	120
5.3.9	Determination and application of the pacific ocean reference sector normalisation	120
5.3.10	Estimation of error or uncertainty (moved to Bioisop)	123
5.4	Validation and comparisons	123
5.4.1	Comparison with standard OMI product	123
5.4.2	Comparison with in-situ measurements	123
5.4.3	Summary	123
5.4.4	Conclusions	123
A	Appendix A	125
A.1	Grid Resolution	125
B	Frequently Asked Questions	127
B.1	How do I change the colors of links?	127
	Bibliography	129

List of Figures

1.1	Ozone production figure copied from [118].	6
1.2	The overall radiative forcings and uncertainties of several atmospheric constituents This is an image taken from [52], found at https://www.ipcc.ch/publications_and_data/ar4/wg1/en/faq-2-1.html	13
1.3	The overall radiative forcings and uncertainties of several atmospheric constituents This is an image taken from [174], chapter 8.	14
1.4	HCHO spectrum, with a typical band of wavelengths used for DOAS path measurements. This is a portion of an image from [37].	17
1.5	Image from [95].	18
1.6	An example spectrum showing interferences used for species concentration measurements by GOME-2. Image by EUMETSAT and ESA ([50].	19
1.7	Standard box model parameters, image taken from [78].	26
1.8	MEGAN schematic, copied from Guenther [65]	29
1.9	Part of a figure from [63] showing global isoprene emission factors. . . .	37
2.1	Surface HCHO simulated by GEOS-Chem with UCX (top left), and without UCX (top right), along with their absolute and relative differences(bottom left, right respectively). Amounts simulated by GEOS-Chem for the 1st of January, 2005.	46
2.2	As figure 2.1, except looking at isoprene.	47
2.3	As figure 2.1, except looking at ozone.	48
2.4	Top panel: surface temperature averaged over January 2005. Bottom panel: surface temperature correlated against temperature over January 2005, with different colours for each gridbox, and the combined correlation. A reduced major axis regression is used within each gridbox (shown in top panel) using daily overpass time surface temperature and HCHO amounts (ppbv). The distribution of slopes and regression correlation coefficients (one datapoint per gridbox) for the exponential regression is shown in the embedded plot.	52
2.5	As figure 2.4 but for northern Australia.	53
2.6	As figure 2.4 but for south-western Australia.	54
2.7	Row 1 shows the tropospheric columns in molec cm ⁻² , GEOS-Chem, OMNO2d, and OMNO2d averaged onto the lower resolution of GEOS-Chem from left to right. Row 2 shows the correlations of GEOS-Chem (X axes) between daily anthropogenic emissions, and mid-day OMNO2d columns. Row 3 shows the differences with OMNO2d columns averaged into the lower resolution of GEOS-Chem.	55

3.1	Ozonesonde release sites and the regions used to examine STT effect on tropospheric ozone levels.	59
3.2	Multi-year monthly median tropopause altitude (using the ozone defined tropopause) determined from ozonesondes measurements at Davis (2006-2013), Macquarie Island (2004-2013), and Melbourne (2004-2013) (solid lines). Dashed lines show the 10th to the 90th percentile of tropopause altitude for each site.	61
3.3	Multi-year mean seasonal cycle of ozone mixing ratio over Davis, Macquarie Island, and Melbourne as measured by ozonesondes. Measurements were interpolated to every 100 m and then binned monthly. Black and red solid lines show median ozone and lapse-rate defined tropopause altitudes (respectively), as defined in the text.	62
3.4	An example of the STT identification and flux estimation methods used in this work. The left panel shows an ozone profile from Melbourne on 8 January 2004 from 2 km to the tropopause (blue dashed horizontal line). The right panel shows the perturbation profile created from band-pass filtering of the mixing ratio profile. The STT occurrence threshold calculated from the 95th percentile of all perturbation profiles is shown as the orange dashed line, and the vertical extent of the event is shown with the purple dashed lines (see details in text). The ozone flux associated with the STT event is calculated using the area outlined with the orange dashed line in the left panel.	64
3.5	Seasonal cycle of STT event frequency at Davis (top), Macquarie Island (middle), and Melbourne (bottom). Events are categorised by associated meteorological conditions as described in the text, with low pressure fronts (“frontal”) in dark blue, cut-off low pressure systems (“cut-off”) in teal, and indeterminate meteorology (“misc”) in cyan. Events that may have been influenced by transported smoke plumes are shown in red (see text for details).	67
3.6	Seasonal distribution of STT events using the alternative STT proxy, obtained from consideration of the static stability at the ozone and lapse rate tropopauses, for Davis (2006-2013), Macquarie Island (2004-2013), and Melbourne (2004-2013).	69
3.7	The distribution of STT events’ altitudes at Davis (top), Macquarie Island (middle), and Melbourne (bottom), determined as described in the text. Events are coloured as described in Fig. 3.5.	70
3.8	The distribution of STT events’ depths, defined as the distance from the event to the tropopause, at Davis (top), Macquarie Island (middle), and Melbourne (bottom), determined as described in the text. Events are coloured as described in Fig. 3.5.	71
3.9	Comparison between observed (black) and simulated (pink, red) tropospheric ozone columns (Ω_{O_3} , in molecules cm^{-2}) from 1 January 2004 to 30 April 2013. For the model, daily output is shown in pink, while output from days with ozonesonde measurements are shown in red. For each site, the model has been sampled in the relevant grid square.	72

3.10	Observed and simulated tropospheric ozone profiles over Davis, Macquarie Island, and Melbourne, averaged seasonally. Model medians (2005-2013 average) are shown as red solid lines, with red dashed lines showing the 10th and 90th percentiles. Ozonesonde medians (over each season, for all years) are shown as black solid lines, with coloured shaded areas showing the 10th and 90th percentiles. The horizontal dashed lines show the median tropopause heights from the model (red) and the observations (black).	73
3.11	Example comparisons of ozone profiles from ozonesondes (black) and GEOS-Chem (red) from three different dates during which STT events were detected from the measurements. The dates were picked based on subjective visual analysis. The examples show the best match between model and observations for each site. GEOS-Chem and ozonesonde pressure levels are marked with red and black dashes respectively. . . .	74
3.12	Top panel: tropospheric ozone attributed to STT events. Bottom panel: percent of total tropospheric column ozone attributed to STT events. Boxes show the inter-quartile range (IQR), with the centre line being the median, whiskers show the minimum and maximum, circles show values which lie more than 1.5 IQR from the median. Values calculated from ozonesonde measurements as described in the text.	77
3.13	(Top) Tropospheric ozone, (<i>I</i>)mpact per event, and (<i>P</i>)robability of event detection per sonde launch, averaged over the region above Davis. The tropospheric ozone column Ω_{O_3} (black, left axis) is from GEOS-Chem, while the STT probability <i>P</i> (magenta, right axis) and impact <i>I</i> (teal, right axis) are from the ozonesonde measurements. The STT impact is multiplied by ten to better show the seasonality. (Bottom) Estimated contribution of STT to tropospheric ozone columns over the region, with uncertainty (shaded area) estimated as outlined in Sect. 3.6. The black line shows STT ozone flux if event lifetime is assumed to be two days, with dashed lines showing the range of flux estimation if we assumed events lasted from one day to one week.	78
3.14	As described in 3.13, for the region containing Macquarie Island.	79
3.15	As described in 3.13, for the region containing Melbourne.	80
4.1	Top panel: isoprene emissions for January, 2005, shown in red, coplotted with tropospheric hcho columns, shown in magenta. Both series are daily averages over Australia. Bottom panel: (RMA) linear regressions from between emissions of isoprene and tropospheric hcho columns, sampled randomly from the 2° by 2.5° latitude longitude gridboxes over Australia for the month of January (2005).	93
4.2	Top row is isoprene emissions for the month of January, in 2005, from GEOS-Chem and estimated from OMI respectively. Bottom row shows the absolute and relative differences between the two.	94
5.1	OMI uncertainty before and after gridding and averaging 8 days from Jan 1 2005 to Jan 8 2005. The third panel shows the number of pixels in each grid box after 8 days of averaging, before accounting for fire. . . .	103

5.2	Solar and viewing zenith angles, image copied from Wikipedia [194], originally from a NASA website.	107
5.3	Column density histograms for a subset of OMI swaths over Australia on the 18th of March 2013. Negative entries are shown in the left panel, positive in the right, note the different scale between negative and positive panels.	113
5.4	Example of grid space change using 0.5x0.5 and 0.25x0.3125 latitude by longitude resolution.	115
5.5	Example of MODIS 8 day grid interpolation from 0.5x0.5 to 0.25x0.3125 latitude by longitude resolution. This example uses MODIS fire counts for 1-8 January 2005.	116
5.6	Vertical column HCHO calculated using OMI satellite swaths with GEOS-Chem aprioris, averaged over 1-8 January 2005 with and without fire affected squares removed.	117
5.7	Constructed example of the initial interpolation of OMI's ω onto a pressure dimension with mismatched surface pressure.	119
5.8	Example of remote pacific reference sector correction (RSC) using 8-day average measurements and one month modelled data. Ω_{VC} shows the uncorrected vertical columns, while Ω_{VCC} shows the corrected vertical columns. OMI corrections shows the correction applied globally based on latitude and OMI track number(sensor). Ω_{GC} shows the GEOS-Chem modelled HCHO VC over the RSC, with Ω_{VCC} showing the corrected VC over the same area.	121
5.9	Example of track correction interpolations for January 1st 2005, points represent satellite slant column measurements, with lines interpolating and extrapolating along the latitudinal direction.	122

List of Tables

3.1	Number of sonde releases at each site over the period of analysis.	60
3.2	Total number of ozonesonde detected STT events, along with the number of events in each category (see text).	66
3.3	Seasonal STT ozone contribution in the regions near each site, in $\text{kg km}^{-2} \text{ month}^{-1}$. In parentheses are the relative uncertainties.	76
4.1	Parameters for each scenario used in CAABA/MECCA model runs. TODO: fill these values in	89
4.2	HCHO yields from various species averaged over Australia during Summer.	95
4.3	HCHO yields from various species, and lifetime against oxidation by OH.	96
5.1	OMI quality flag values table from Kurosu and Chance [89]	112
A.1	The 47 level vertical grid used by GEOS-Chem	126

Chapter 1

Introduction and Literature Review

1.1 The atmosphere

The atmosphere is made up of various gases held to the earth's surface by gravity. These gases undergo transport on all scales, from barbeque smoke being blown into your face to smoke plumes from forest fires travelling across the world and depositing in the antarctic snow. They take part in various chemical reactions along the way, largely driven by solar input and interactions with each other. Various chemicals are lofted into the atmosphere by soil, trees, factories, cars, seas and oceans, you name it. They are also deposited back to the surface both directly and in rain drops.

Mostly the atmosphere is made up of nitrogen (N_2 : $\sim 78\%$), oxygen (O_2 : $\sim 21\%$), and argon (Ar : $\sim 1\%$). Water (H_2O) ranges from 0.001 to 1% depending on evaporation and precipitation. Beyond these major constituents the atmosphere has a vast number of *trace gases*, including carbon dioxide (CO_2 : $\sim 0.4\%$), Ozone (O_3 : 0.000001 to 0.001%), and methane (CH_4 : $\sim 0.4\%$) [BrasseurJacob2017]. Trace gases in the atmosphere can have a large impact on living conditions. They react in complex ways with other elements (anthropogenic and natural), affecting various ecosystems upon which life depends.

Most of the atmosphere ($\sim 85\%$) is within 10 km of the earth's surface. This is due to air pressure, which decreases logarithmically with altitude.

1.1.1 Structure

1.1.2 Chemistry

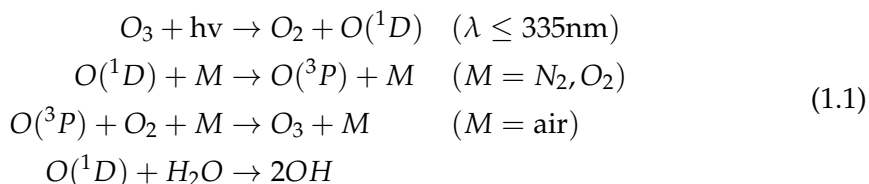
Hydroxyl radicals

The OH radical drives many processes in the atmosphere, especially during the day when photolysis of ozone drives OH concentrations [10]. OH is a key species which reacts with nearly all the organic compounds in the troposphere. The exceptions are chlorofluorocarbons (CFCs), and Halons not containing H atoms [10]. OH and HO_2 concentrations largely determine the oxidative capacity of the atmosphere. Oxidation and photolysis are the two main processes through which VOCs are broken down into HCHO, O_3 , CO_2 and various other species. Over land, isoprene (C_5H_8) and monoterpenes ($\text{C}_{10}\text{H}_{16}$) account for 50% and 30% of the OH reactivity respectively [56].

In the late 90's it was thought that OH radicals are formed exclusively from photolysis of O_3 , HONO, HCHO, and other carbonyls ($\text{R}_2\text{C}=\text{O}$) [10]. Isoprene (C_5H_8) was

thought to be a sink of OH until it was shown by [144] that the radicals are recycled. This recycling process is discussed in more detail in section 1.3.3.

Ozone is an important precursor to HO, as excited oxygen atoms ($O(^1D)$) are created through photolysis, which then go on to mix with water and form OH, as shown in this equation taken from [10]:

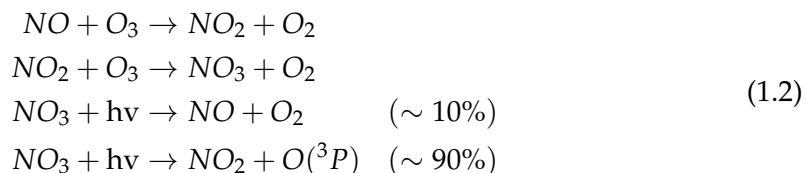


This shows how some of the $O(^1D)$ recycles back to Ozone, while some forms OH. NB: The wavelength was updated to 350 nm in [11].

Ozone is also a very important substance for formation of radicals (NO_3 , OH) in the troposphere through photolysis in the presence of water.

Nitrate radicals

Nitrate radicals NO_3 are largely formed through ozone reactions. They are photolysed very rapidly during the day, with a lifetime of about 5 s [10]. If NO and O_3 are both in the atmosphere, the following reactions [10] occur:



A build up of NO_3 radicals can be seen at night, when photolysis is not removing them quickly [10, 24].

Since radicals play such a big role in regulating many chemical reactions in the atmosphere it's important for models to accurately represent them (eg. [Travis2014]). This is difficult as they are coupled with so many other species and measurements of OH are not readily available on a global scale.

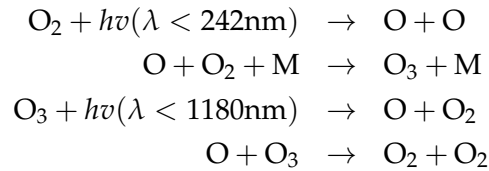
Ozone in the lower atmosphere is a serious hazard that causes health problems [73], damages agricultural crops worth billions of dollars [12, 202], and increases the rate of climate warming [130].

1.2 Ozone

Ozone (O_3) is mostly located in the stratosphere, where it helpfully prevents much of the shorter wave length solar radiation from reaching the earth's surface (ie UV light). However around 11% of the total column of ozone is located in the troposphere (TODO: cite), where it has several deleterious effects. Around 5 to 20 percent of all air pollution related deaths are due to ozone ([126]). In the short term, ozone concentrations of ~ 50 -60 ppbv over eight hours or ~ 80 ppbv over one hour are agreed

to constitute a human health hazard [13, 97]. Long term exposure to lower levels cause problems with crop loss and ecosystem damage [9], and both short and long term concentrations may get worse in the future [97, 173]. Further tropospheric ozone enhancements are projected to drive reductions in global crop yields equivalent to losses of up to \$USD₂₀₀₀ 35 billion per year by 2030 [12], along with detrimental health outcomes equivalent to ~\$USD₂₀₀₀11.8 billion per year by 2050 [158]. Recently [202] showed that the net effect of near-surface ozone on is a ~ 14% decrease in net primary productivity (NPP) in China, which could be reduced by ~ 70% with drastic measures by 2030.

In the stratosphere ozone production is generally driven by the Chapman mechanism, as high energy light (with wavelengths $\lambda < 242$ nm) photolyses the molecular oxygen (O_2) in the atmosphere [BrasseurJacob2017]. The Chapman mechanism involves several equations which lead to rough equilibrium of O, O_2 , O_3 and pressure, as follows:



Where hv represents radiation and M is an inert molecule (such as N_2). The high energy photons ($\lambda < 242$ nm) are present from the top of the atmosphere but are mostly removed before reaching the troposphere. The lifetime of O against loss by O_2 is less than a second in the troposphere, and produced O_3 quickly returns to O and O_2 , as low energy ($\lambda < 1180$ nm) light and M are abundant. The gradient of light penetration in addition to the logarithmic decrease in atmospheric pressure (which affects M abundance) drives (using the Chapman equation) the vertical profile of ozone into what is called the ozone layer, where most of the ozone is in the stratosphere. This mechanism requires radiation so only takes place during the daytime, during the night there are different processes driving ozone chemistry.

Smoke plumes from biomass burning can carry ozone precursors, creating higher ozone concentrations downwind of the plume's source. Fire emissions include a range of chemicals and each year the affects of fire or burning seasons blanket the northern and southern hemispheres independently.

TODO: get access to Hegglin (10.1038/ngeo604) [69]

Since the Montreal Protocol on Substances that Deplete the Ozone Layer was established in August 1987, and ratified in August 1989, several satellites and many measurement stations were set up to monitor ozone in the stratosphere. However, in the southern hemisphere there are relatively few records of ozone ([75]). One method of measuring ozone in the troposphere and stratosphere is by releasing weather balloons (with attached ozone detectors) which take readings as they rise up to around 30 km, giving a vertical profile of concentrations. Since 1986, Lauder, New Zealand (45°S, 170°E) has released ozonesondes allowing a multi-decadal analysis of ozone concentrations over the city [23]. Kerguelan Island (49.2°S, 70.1°E), also has a record of ozonesonde profiles, which are directly in the path of biomass burning smoke plumes

transported off shore from Africa [15]. SHADOZ is the southern hemispheric additional ozone project, which have released sondes from 15 sites at different times <http://tropo.gsfc.nasa.gov/shadoz/>.

What drives ozone in the troposphere? Two main contributors are transport from the stratosphere and creation due to biogenic emissions of precursors. At smaller (regional) scales anthropogenic emissions are also important, especially in large cities such as Sydney due to NO_x emissions from traffic and power production.

1.2.1 Stratosphere to troposphere transport

Historically (in the late 1990's), ozone transported down from the stratosphere was thought to contribute 10-40 ppb to tropospheric ozone levels, matching tropospheric production [10, 175]. This number was revised down over the years as measurement and modelling campaigns improved our understanding of global scale transport, mixing, and chemistry [126]. Recently [88] analysed various measurements in south-east USA and observed STT influence which can be seen to affect surface ozone levels. In their work they use high spectral resolution lidar (HSRL), ozonesondes, ozone lidar, and airborne in-situ measurements give the structure and temporal evolution of ozone and the low front weather system.

Ozone transported to the troposphere from the stratosphere can occur through diffusion (slow process (TODO: Cite)) or through mixing, often called Stratosphere to Troposphere Transport events (STT), or intrusions. TODO: compare these two processes and their impacts briefly. Recently global chemical transport models (CTMs) have been used to trace how much ozone is being transported to the troposphere from the stratosphere. There are a few methods of doing this, such as [135], who use the ECHAM5 CTM with a tracer that keeps track of ozone formed and transported from the stratosphere. Model based estimates generally require validation against actual measurements, such as those from ozonesondes or satellites. [69] estimate that climate change will lead to increased STT due to an acceleration in the Brewer Dobson circulation. They estimate ~ 30 , and $\sim 121 \text{ Tg yr}^{-1}$ increases (relative to 1965) in the southern and northern hemispheres respectively

[107] examine southern hemispheric ozone and the processes which control its inter-annual variability (IAV). IAV is the standard deviation of ozone anomalies (difference from the monthly mean). They show that ozone transported from the stratosphere plays a major role in the upper troposphere, especially over the southern Indian ocean during austral winter. While stratospheric transport mostly impacts the upper troposphere, some areas are impacted right down to the surface. [107] look at modelled tropospheric ozone sensitivity to changes in stratospheric ozone, ozone precursor emissions, and lightning over the southern hemisphere from 1992–2011. Their work suggest ozone at 430 hPa is mostly stratospheric in September over 20°S to 60°S at all longitudes. They also see tropospheric ozone sensitivity to emissions from South America ($0\text{--}20^\circ\text{S}$, $72.5\text{--}37.5^\circ\text{W}$), southern Africa ($5\text{--}10^\circ\text{S}$, $12\text{--}38^\circ\text{E}$), and South to South-east Asia ($70\text{--}125^\circ\text{E}$, $10^\circ\text{S}\text{--}40^\circ\text{N}$). In the USA recent work by [103] suggests that intrusions during spring are increasing surface ozone levels. Their work also recommends that understanding of frequency and cause of STT needs to be improved to effectively implement air quality standards.

An analysis of the Atmospheric Chemistry and Climate Model Inter-comparison Project (ACCMIP) simulations by [200] found STT is responsible for $540 \pm 140 \text{ Tg yr}^{-1}$, equivalent to $\sim 11\%$ of the tropospheric ozone column, with the remainder produced photochemically [126].

1.2.2 Chemical production

The tropospheric ozone concentrations rely on climate and ozone precursor emissions; including NO, NO₂, CO, VOCs, and HCHO [Marvin2017, 10, 200]. Ozone predictions are uncertain and difficult due to the vagaries of changing climate which affects both transport, deposition, destruction, and plant based precursor emissions. All of these processes are tightly coupled and difficult to accurately model, as they depend on uncertain assumptions such as CO₂ dependency [200]. Even with all the work done in the prior decades there remains large uncertainties about ozone precursors in the troposphere [118].

Ozone is formed in the troposphere through oxidation of VOCs in the presence of NO_x. VOCs are described in the following section (Section 1.3). Net formation or loss of O₃ is determined by interactions between VOCs, NO_x, and HO_x, and is a complicated system of positive and negative feedbacks [10]. Figure 1.1 shows the non-linear affect of NO_x and VOC concentrations on ozone production over Houston, as modelled in [118]. Recently the relationship has been examined on the intradiel timescale showing that ozone production can be more or less sensitive to VOCs at different hours depending on location various other factors [118].

Ozone in rural areas is often higher than in populous cities, as the high NO levels titrate the O₃. Equation 1.2 shows how NO and O₃ lead to NO₂ and the very short lived NO₃ radical.

Tropospheric ozone is lost via chemical destruction and dry deposition, estimated to be $4700 \pm 700 \text{ Tg yr}^{-1}$ and $1000 \pm 200 \text{ Tg yr}^{-1}$, respectively [172]. The main loss channel is through equation 1.1, where photolysis and pressure create OH from the O₃.

1.3 VOCs

Organic compounds are members of a large class of chemicals whose molecules contain carbon, with the exception of a few compounds such as carbides, carbonates (CO₃), and simple oxides of carbon and cyanides. Organic compounds can be categorised based on their vapour pressure, which is the tendency of a liquid or solid to vaporise. Compounds with high vapour pressures at standard temperature are classed as volatile, and have a felicity to evaporate at low temperatures. Plants contain tens of thousands of organic compounds, it's likely that fewer than 40 are emitted due to the low volatility of most of them [67].

Atmospheric organic compounds are legion and differ by orders of magnitude with respect to their fundamental properties, such as volatility, reactivity, and cloud droplet formation propensity. Volatile organic compounds (VOCs) have vapour pressure greater than 10^{-5} atm , and are mostly generated naturally by plants, which emit

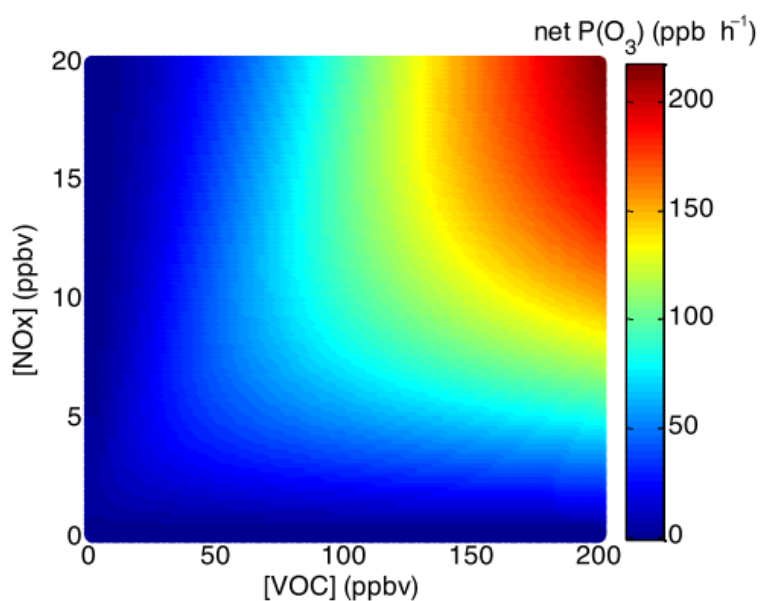


Figure 1. Ozone production empirical kinetic modeling approach (EKMA) diagram using box model results with NO_x levels varying from 0 to 20 ppbv and VOC levels from 0 to 200 ppbv. The mean concentrations of other species and the speciation of NO_x and VOCs observed during DISCOVER-AQ in Houston in 2013 were used to constrain the box model. This diagram clearly shows the sensitivity of ozone production to NO_x and VOCs in Houston.

FIGURE 1.1: Ozone production figure copied from [118].

around 1000 Tg yr⁻¹ [66, 60]. Due to their high volatility these compounds are generally seen in the gas phase. Organic compounds with a lower volatility are classed as semi-volatile (SVOCs: vapour pressure between 10⁻⁵ and 10⁻¹¹ atm) are seen in both gas and particle phase depending on temperature and pressure. Organic compounds with even lower vapour pressure are generally found in the particle phase in aerosol particulate matter [60]. Understanding the drivers of trends in biogenic VOC emissions (BVOCs) is needed in order to estimate future carbon fluxes, changes in the water cycle, air quality, and other climate responses [201].

VOCs are an important driver of atmospheric processes, especially near forests. VOC emissions result in radical cycling, acid deposition, production of tropospheric ozone, and secondary organic aerosols (SOAs) [10, 84]. A regional-model study in Europe ([4]) has also shown VOCs impact secondary inorganic aerosol concentrations. These have impacts on climate (through radiative forcing) and air quality, affecting both human health and crop yields [52, 12, 98].

The major source of VOCs in the atmosphere is biogenic, with around 90% of emissions (globally) coming from natural sources [66, 63, 123]. Global non-methane VOC (NMVOC) levels are estimated at 85 %, 13 %, and 3 % from biogenic, anthropogenic, and pyrogenic sources respectively [85]. Methane and isoprene each comprise around a third of the global total emissions of VOCs ([63]). However, methane is relatively long lived (years) and is well mixed in the atmosphere while isoprene levels are very volatile and spatially diverse due to a life time of around an hour. This means that methane measurements and concentrations are relatively well understood, while NMVOCs are less so.

VOCs are removed by wet and dry deposition, OH oxidation, reaction with NO₃, ozonolysis (at night time or in polluted areas) or photolysis [11, 24]. The process of deposition only accounts for a small fraction of the VOC loss, with the possible exception of the long lived methane compound [11].

PM in the atmosphere is a major problem, causing an estimated 2-3 million deaths annually [71, 86, 160, 98]. Aerosols are suspended particulates and liquid compounds in the atmosphere, of which particulate matter (PM) is an important subset. Fine particulate matter (PM_{2.5}) penetrates deep into the lungs and is detrimental to human health. Some PM comes from small organic aerosols (OA) emitted in the particulate phase and referred to as primary OA (POA). A substantial amount of PM is due to gaseous organic compounds transforming in the troposphere leading to what's known as secondary OA (SOA) [87].

Formation of SOA is generally due to VOC oxidation and subsequent reactions, while removal from the atmosphere is largely due to wet or dry deposition, and cloud scavenging [84]. It can be difficult to attribute PM formation, in part due to the complex relationship between NO_x, OH, O₃, and the uncertainty surrounding precursor emissions.

1.3.1 Isoprene

Isoprene, or 2-methylbuta-1,3-diene, is a VOC with the chemical formula C₅H₈. It is of major importance to the atmosphere, as it is involved in various processes which alter the oxidative capacity of the atmosphere. NMVOCs are alkanes, alkenes, aromatic

hydrocarbons and isoprene, with isoprene being the most prominent. [66], and subsequent updates [67, 63, 64], have been used ubiquitously by the atmospheric community as a global estimate of isoprene emissions, at roughly 500-600 Tg yr⁻¹, emitted mostly during the day. Recently an estimate of global isoprene emissions has been made using a completely different model, of around 465 Tg C yr⁻¹, by [119] using ORCHIDEE. The global emission factors model used to derive both these estimates is based on modelling emissions from different plant species (phenotypes), and relatively few Australian species are used when forming in these estimates.

Isoprene affects NO_x and HO_y cycling, see for example formulae 1.1, 1.2. In the presence of NO_x, isoprene forms tropospheric ozone and SOAs [191, 123]. It has a short lifetime during the day, roughly an hour due to OH oxidation [11]).

Measurements of isoprene are often uncertain or difficult to make accurately. [84] summarised how chamber experiments used to measure isoprene reactions may be unsuitable for comparison to the natural atmosphere. In [Nguyen2014] many scientists and groups worked together on chamber measurements, to improve understanding of ambient atmospheric oxidation mechanisms of biogenic hydrocarbons (such as isoprene).

Major emitters are tropical broadleaves (notably eucalypts), and scrubs [63, 7, 134, 126]. It used to be thought that emissions of anthropogenic and biogenic VOCs (AVOCs, BVOCs respectively) were roughly similar ([129], TODO: more cites). Methane (CH₄) is one of the more abundant and potent VOCs, however it is often classified separately and compared against non-methane VOCs (NMVOCs). In the 1990's it became clear that biogenic emissions of VOCs were in fact dominant, although methane emissions are still largely anthropogenic.

1.3.2 Emissions

Isoprene emissions are often classified as either anthropogenic, biogenic, or pyrogenic. The natural or biogenic sources are roughly ten times higher than the anthropogenic VOC sources [63, 84]. BVOC emissions make up 87% of NMVOC emissions [84, 85].

The World Meteorological Organisation (WMO) estimated that we are emitting 360 Mt yr⁻¹ of methane, compared to biogenic emissions of around 200 Mt yr⁻¹ [10]. In 1995 emissions of other VOCs were estimated at 1150 Tg C yr⁻¹ from biogenic sources, and 100 Tg C yr⁻¹ from anthropogenic sources [66, 10]. The main non-methane BVOC emissions are isoprene (44%) and monoterpenes (11%) ([67, 85]). Land use changes can drastically affect isoprene sources, for instance in the tropics where large scale deforestation has converted forest into crop lands [84].

Biogenic VOC emissions affect surface pollution levels, potentially enhancing particulate matter (PM) and ozone levels.

Isoprene is emitted and enters the atmosphere in the gas phase, where it reacts with various chemicals, forming many new chemicals with reactions at various time scales. One common compound which is produced by these reactions is HCHO, which is easier to measure and often used to estimate how much isoprene is being emitted. The estimated yield of HCHO is but one aspect of the many processes going on in this space. There are many reactions which occur and are important to capture in models due to their impacts on air quality and physical properties in the lower atmosphere.

The many children processes and products which begin with isoprene oxidation are often called the isoprene (photochemical) cascade [Paulot2012, 31, 199].

1.3.3 The isoprene cascade

Isoprene forms many products with various lifetimes, here I will present an overview of some important mechanisms and products which are useful to my work.

Photolysis and oxidation of many VOCs initially form alkyl radicals (\dot{R}).

Alkenes (VOCs with double bonded carbon, such as isoprene) react with ozone leading to organic peroxy radicals ($RO\dot{O}$). These go on to form many products and lead to (amongst other things) aerosol, formaldehyde, and ozone formation, depending on various other factors such as sunlight and NO pollution [10].

Oxidation

The primary first step for atmospheric isoprene is photooxidation, reacting with OH to form isoprene hydroxyperoxy radicals (ISOPOO, or ROO, or $RO\dot{O}$) ([Marvin2017, Patchen2017, 199]). There is still uncertainty about which pathways are most important following ISOPOO production: HO_2 reactions predominantly produce hydroxyhydroperoxides (ISOPOOH), NO reactions largely produce methyl vinyl ketone (MVK) and methacrolein (MCR), and RO_2 reactions are also possible [108].

The first step in oxidising alkenes (including isoprene) is a replacement by OH of a double bond, as summarised by the equation from [142]: $R-CH=CH-R' + OH \longrightarrow R-CH(OH)CH-R'$ where R and R' represent hydrocarbons. This OH adduct then reacts with O_2 to produce a hydroxyperoxy radical ($RO\dot{O}$), which for isoprene can be any of six different isomers [142]. This is where the isoprene oxidation path splits depending on the NO_x concentration. Reactions with NO can lead to ozone production in both isoprene and other non-methane organic compounds (NMOCs) and NMVOCs ([142, 11]). These reactions are complex and coupled, for example NO_2 concentrations can be increased by NMOC and NO reactions [11].

Reaction with NO_2 forms hydroxynitrate ($RONO_2$), also known as peroxyacetyl nitrate (PAN). The first generation of organic nitrates produced by isoprene oxidation range from 7% to 12%, shown in laboratory experiments [143, 111]. A portion of isoprene nitrates are recycled back to NO_x , so may serve as a reservoir of nitrogen and allow its transport to the boundary layer of remote regions ([142, 143]). [142] examine this branching step where isoprene either forms ROO or $RONO_2$, and for specific conditions they determine the reaction rates for each branch. They find the most frequent pathway is the formation of ROO (99.3%). Although the PAN formation branch is quite minor, it can be very important. PAN can transport NO_x to otherwise clean regions ([72]), and can build up in the winter [97]. PAN has a relatively long lifetime (against OH, order of 1 day) and is able to transport and release the NO_x in environments which are quite far from any emissions. This transport can be exacerbated by fast winds and low OH concentrations, which makes PAN an important factor in modelling atmospheric chemistry.

The oxidation products of isoprene through OH adduction (forming ISOPOO) followed by addition of O_2 produces various isomers of alkylperoxyl radicals (organic

peroxyl radicals, or RO_2), which react with HO_2 or NO and produce stable products (often called oxidised VOCs or OVOCs) [Nguyen2014]. The ISOPOO radicals are eventually destroyed by NO , HO_2 and other RO_2 , with most pathways potentially producing HCHO [199]. Oxidation reactions are important and quickly stabilise the ratio of NO to NO_2 . NO_x is removed primarily by conversion to nitric acid (HNO_3) followed by wet or dry deposition [13]. There is still large uncertainty around the fate of various RO_2 radicals, which limits understanding of the relative importance of some chemical processes [32].

Some portion of emitted isoprene leads to SOA, potentially through the formation of methacrylic acid epoxide (MAE) formed by decomposition of methacryloylperoxynitrate (MPAN, a second generation product of isoprene oxidation) as shown in smog chambers and field studies in [104]. In the presence of NO_x , the ISOPOO radicals ($\text{ROO}\cdot$) form organic nitrates after reacting with NO . Any organic nitrates which are formed affect levels of both HO_x (H , OH , peroxy radicals) and NO_x , acting as a sink ([111] and references therein).

Isoprene oxidation by OH is less well understood when lower concentrations of NO are present in the atmosphere. Initially isoprene was thought to be a sink for atmospheric oxidants [e.g. 67]. It was thought that in low NO environments, like those far from anthropogenic pollution and fires, oxidation of isoprene would create ISOPOOH and lead to low concentrations of OH and HO_2 [144]. In [144], the HO_x levels are shown to be largely unaffected by isoprene concentrations. They show that ISOPOOH is formed in yields $> 70\%$, and MACR and MVK is formed with yields $< 30\%$. The formation of MACR and MVK produces some HO_x , although not enough to close the gap. [144] goes on to suggest (and provide experimental evidence) that dihydroxyperoxides (IEPOX) are formed from oxidation of the ISOPOOH, which form precursors for SOAs as well as closing the HO_x concentration gap. They then use GEOS-Chem, modified to include IEPOX formation, to estimate that one third of isoprene peroxy radicals react with HO_2 , and two thirds react with NO . They estimated $95 \pm 45 \text{ Tg yr}^{-1}$ IEPOX being created in the atmosphere, which (at the time) was not modelled by CTMs. Their work showed another pathway for isoprene based SOA creation, through these IEPOX creation and HO_x recycling mechanisms. [145] suggested that the work of [144] only partially bridges the gap between clean air HO concentration measurements and models. They suggested four new mechanisms for OH recycling in these pristine conditions. These can be summarised as OH regenerating reactions which occur during photolysis of hydroperoxy-methyl-butenals (HPALDs), and resulting photolabile peroxy-acid-aldehydes (PACALDs). These reactions are highly non-linear and subject to large uncertainty, however when compared against several campaigns they were shown to improve one particular models (IMAGES) HO_x concentrations. In [31], MACR products are examined in various conditions and hydroxy recycling is also observed in low NO conditions.

Although understanding of OH production/recycling in these low NO conditions has been improved, many observations of OH are still quite under-predicted in models [110]. [110] showed how traditional OH measurements may be overestimated due to VOC oxidation. They looked at measurements in a remote forest in California and found that the instruments were generating OH internally. [Nguyen2014] also see this VOC oxidation interference in measurements using a gas chromatographer (GC)

with an equipped flame ionisation detector (FID). This lends more credence to the current understanding of VOC oxidation as it closed the gap between measurements and model predictions ([110]).

[145] showed that HO_2 is produced at near unity yields following isoprene oxidation initiated by HO. TODO: read more Peeters2010

[Nguyen2014] examine various measurement techniques to determine isoprene reactions in non-laboratory conditions. Their work discussed how large uncertainties persist in isoprene oxidation, which carries through to predictions by atmospheric models. [Nguyen2014] show preliminary estimates of low-NO yields of MVK and MCR to be $6 \pm 3\%$ and $4 \pm 2\%$ respectively, consistent with TODO:[Liu2013], but only when cold-trapping methods are employed. These yields each increase (due to interference by OVOCs) to greater than 40% when directly sampled by GC-FID.

During the night isoprene is oxidised by NO_3 radicals, which joins to one of the double bonds and produces organic nitrates in high yield (65% to 85%) [111]. (todo: read mao2013 para 3 cites) These organic nitrates go on to produce further SOAs, largely due to NO_3 reacting with first generation isoprene oxidation products [152]. [152] examine SOA production in a large chemical reaction chamber, over 16 hr in the dark and find first generation mass yield ($\Delta\text{SOA mass} / \Delta\text{isoprene mass}$) to be less than 0.7%, with further oxidation of initial products (isoprene reacting twice with NO_3) yielding 14%. This led to an overall mass yield of 2% over the 16 hr experiment.

Even with the recent boom in isoprene analysis, uncertainties remain in the isoprene oxidation mechanisms. Examples (taken from [Nguyen2014]) include isoprene nitrate yields, which range from 4-15% [143], 90% disagreements in MAC and MVK yields TODO:[Liu2013], various possible sources for SOA TODO:[Chan2010, Surratt2010, 104], unknown HPALD fates, incomplete O_2 incorporation TODO:[Peeters2009, 32], and under-characterized RO_2 lifetime impacts TODO:[Wolfe2012]. TODO: get those citations and read abstracts.

Ozonolysis

Ozonolysis is the splitting of carbon chains by ozone molecules, and is among the primary oxidation pathway for volatile alkenes [132]. Criegee intermediates (carbonyl oxides with two charge centres) are formed when isoprene reacts with O_3 . [132] examine in detail a few of these, with proposed mechanisms for C_1 and C_4 Criegee intermediate reactions. The C_1 stabilised Criegee (CH_2OO , $\sim 61\%$) is therein proposed to react with water yielding 73% hydroxymethyl hydroperoxide (HMHP), 6% $\text{HCHO} + \text{H}_2\text{O}_2$, and formic acid + H_2O , and the same products with yields of 40, 6, and 54% respectively when this Criegee reacts with $(\text{H}_2\text{O})_2$. TODO: more on Nguyen2016?

SOA

Gas phase emissions with higher vapour pressures can be oxidised into lower vapour pressure products which will partition between gas and particle phase, often called semi or non-volatile. The aerosol products from these gas phase emissions (or the children thereof) are called SOA [84]. In the [84] review of global SOA science, uncertainty in radiative forcing of aerosols is highlighted, and 20-90 % of PM mass in

the lower troposphere is OA. Less volatile OA also plays a role, although PM production from this source is complicated and makes up only a small fraction ($\sim 1\%$) of the resulting PM ([87, 20]). Modelling OA has many uncertainties due to the complexity of SOA formation and various pathways such as aqueous phase oxidation which can significantly contribute to concentrations. This is further hindered by poor understanding of precursor emissions, and lumping together various compounds, of which only some form SOA (for example ORVOCs in GEIA (back in 2005)). Satellite data requires SOA models to estimate a full vertical profile of aerosols for remote sensing techniques [84].

SOA formation from VOCs in atmospheric CTMs is generally imperfect due to the complicated chemistry and diverse nature of atmospheric conditions. Yields of SOA from VOCs are often lumped together and based on empirical laboratory chamber data. VOC oxidation was not feasible ~ 12 years ago (2005), as chamber studies did not extend over a large enough parameter range and the importance of heterogeneous aerosol chemistry on SOA formation was unquantified [84].

One of the large uncertainties with OA is the total effect on radiative forcing, 12 years ago it was well understood that most OA cool the atmosphere, with smaller particles having a larger affect due to the size matching the wavelengths of visible light [84]. Transport and indirect effects complicate matters further, with cloud creation and modification of cloud properties being quite difficult to accurately predict. In the third IPCC report [77], the uncertainty involved if OA forcing was a factor of 3 times the estimated effect. This has since been improved however OA and cloud formation still remains a large uncertainty in more recent IPCC reports [52]. Figure 1.2 shows the radiative forcing (RF) of various atmospheric constituents, it's clear that OA uncertainty dominates. Figure 1.3 shows the same summary updated in chapter 8 of the fifth report, where the SOA uncertainty remains quite large. It's currently understood that SOA plays an indirect and complex role in cloud properties, with a net cooling effect [174, Chapter 7,8]

(TODO: read more of Kanakidou2005) The emissions of precursors to SOA was and is quite uncertain, in [84] they state that these uncertainties range from a factor of 2 to 5. They highlight emissions and flux measurements as well as implementing satellite data in models as a means of improving the emissions inventories. In 2005, (as of [84],) the knowledge gaps in isoprene and terpene oxidation processes included precursor gases to SOA, impact of NO_x on SOA formation, heterogeneous reactions between particles and gaseous compounds, aqueous phase chemistry, and complete aerosol compositions. At this time SOA driven nucleation was under debate, as chamber studies showed that SOA led to new particles but only in the particle free laboratory setting. Nucleation of new particles was suppressed by condensation if any seed aerosol was already present. Observed nucleation outside of laboratories was suggested to have arisen from biogenic SOAs, driven by ozonolysis. [84] concluded that it is very likely that organics contribute to particle growth and formation rates.

Night time chemistry

At night when OH concentrations have dropped, isoprene can remain in the atmosphere to be transported. Typically less than half of this night time isoprene is removed through ozonolysis [11], however, in polluted areas where high levels of NO_x

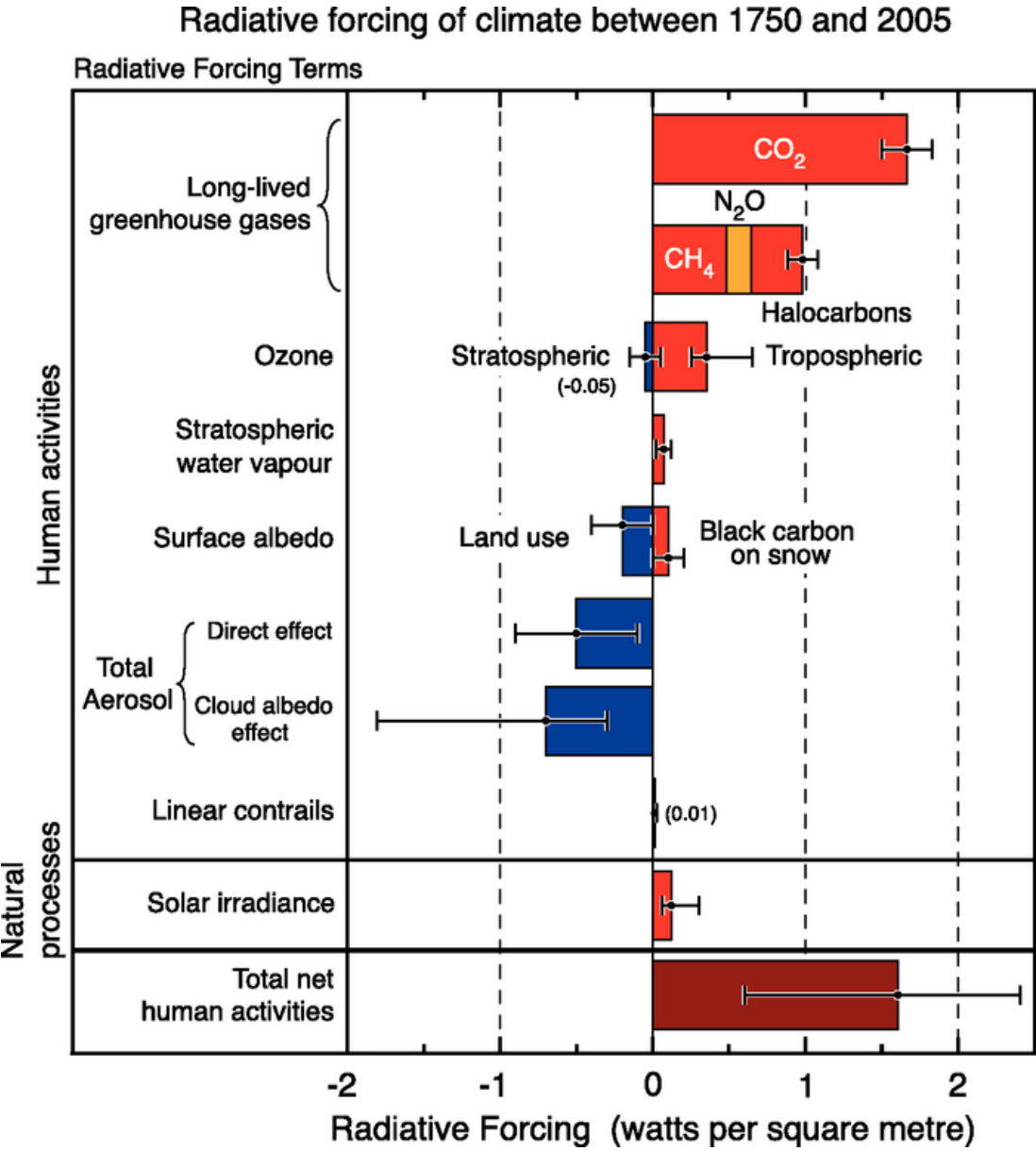


FIGURE 1.2: The overall radiative forcings and uncertainties of several atmospheric constituents This is an image taken from [52], found at https://www.ipcc.ch/publications_and_data/ar4/wg1/en/faq-2-1.html.

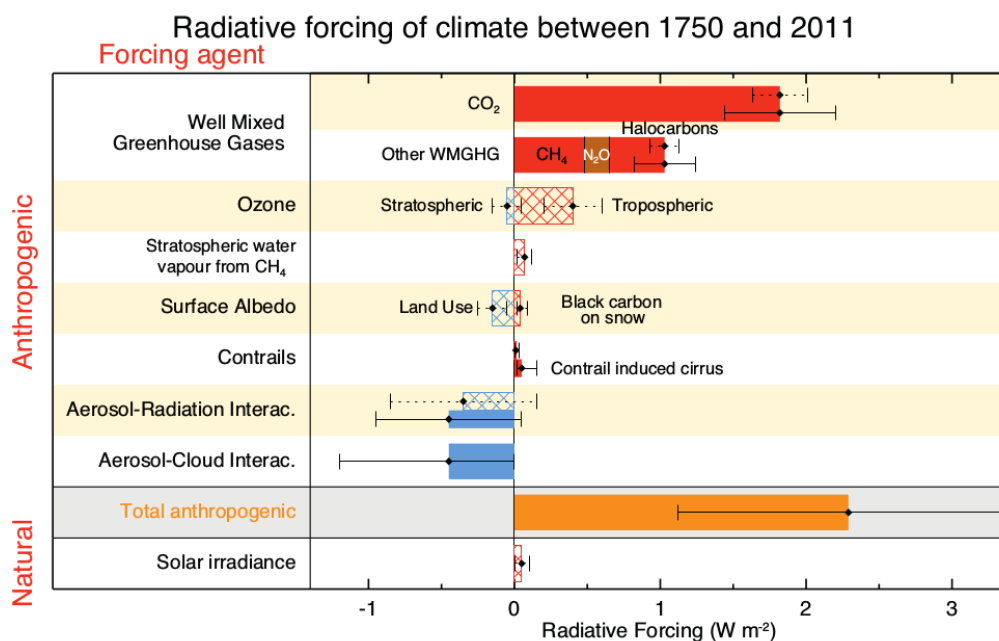


Figure 8.15 | Bar chart for RF (hatched) and ERF (solid) for the period 1750–2011, where the total ERF is derived from Figure 8.16. Uncertainties (5 to 95% confidence range) are given for RF (dotted lines) and ERF (solid lines).

FIGURE 1.3: The overall radiative forcings and uncertainties of several atmospheric constituents This is an image taken from [174], chapter 8.

exist, isoprene is consumed by a different radical. During the night time, nitrate radicals (NO_3) build up, especially in areas with high NO_x levels. In areas with high NO_x levels, greater than 20% of the isoprene emitted late in the day ends up being oxidised by the NO_3 radical over night [24]. So while night time isoprene is not as highly concentrated, it does have varying biogenic and anthropogenic sinks. At night isoprene has effects on both NO_x concentrations and ozone levels, and can form harmful SOAs [24, 111]. The night-time concentrations of OH and ozone also have a complex effect on NO_x removal in high latitude winters, when photolysis and NO reactions are reduced [13].

One of the major products of isoprene chemistry is HCHO. HCHO is important both for its own sake, and as a proxy for determination of isoprene emissions.

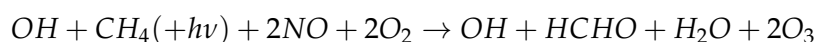
1.4 HCHO

HCHO, aka methanal, methyl aldehyde, or methylene oxide, is of the aldehyde family. HCHO is an OVOC which is toxic, allergenic, and a potential carcinogen. It is dangerous at low levels, with WHO guidelines for prolonged exposure at 80 ppb. HCHO is used as an adhesive in plywood, carpeting, and in the creation of paints and wallpapers. Emissions in enclosed spaces can build up to dangerous levels, especially if new furnishings are installed ([37]). At global scales HCHO in furniture is less important, as concentrations are driven by photochemical reactions with methane and other VOCs.

[124] show that anthropogenic emissions of HCHO in America are mostly negligible, although improved sensitivity from oversampling allowed satellite detection of enhanced HCHO concentrations over Houston and Texas [208]. This is not the case in China, since massive population centres and industrial districts are emitting huge amounts of VOCs into the atmosphere [55]. [55] use GOME measurements over Asia and derive biogenic, anthropogenic, and pyrogenic VOC emissions, and [208] use oversampling of the OMI HCHO measurements to determine anthropogenic highly-reactive VOC emissions. Then with their updated emissions they show how surface ozone is affected, with a seasonal increase of 5-20 ppb simulated by GEOS-Chem.

1.4.1 Sources and sinks

In the atmosphere HCHO is primarily produced through the oxidation of methane (CH_4) by the hydroxyl radical (OH). [10] summarised the background formation of HCHO with the following reaction:



which shows that photolysis and oxidation of methane forms HCHO and ozone in a process that regenerates the OH radicals. CH_4 concentrations are thought to be well constrained in models, with the ACCMIP comparison showing only $\sim 3\%$ inter-quartile range ([200]). There is a complex relationship between VOCs, HO_x , and NO_x , and with higher levels of NO_x the speed that VOCs are converted into HCHO increases, as does the HCHO concentration ([199]).

Within the continental boundary layer, the major source of HCHO enhancement is VOC emissions reacting with OH radicals in the presence of NO_x ([191, 123, 85]). Enhancements to regional and continental HCHO are largely driven by isoprene emissions ([66, 139, 159, 85]). This is true except near fires or anthropogenic sources of HCHO and precursors ([66, 85, 199]). Biomass burning (BB) can be a source of HCHO, and various other pollutants, precursors, and aerosols ([66, 6]). Additionally HCHO is emitted into the atmosphere directly through fossil fuel combustion, natural gas flaring, ethanol refining, and agricultural activity ([199]).

Other terpenoids (monoterpenes, sesquiterpenes, etc.) can also produce HCHO, although generally to a lesser extent than isoprene, methane and biomass burning ([64]). Many of the HCHO yields from terpenoids are estimated through chamber studies which examine the products molecular mass and charge after mixing the compound of choice into a known volume of air ([Nguyen2014]). These conditions generally don't match those of the real world, where ambient air will have a cocktail of these compounds as well as various reactants. [Nguyen2014] state that one of their goals is to recreate ambient atmosphere in their chamber studies with more accuracy, in order to improve interpretations and allow more accurate model parameters.

In the past, HCHO levels were underestimated by models, often with large discrepancies, due to the poor understanding of methyl peroxy radical (CH_3OO) chemistry ([191]). Nowadays HCHO concentrations are better understood, however precursor emissions are one of the main unknowns ([Marvin2017, 48, eg.]). [Marvin2017] found that discrepancies in modelled HCHO concentrations are primarily due to second and later generation isoprene oxidation chemistry.

HCHO has two major sinks, one being reactions with OH (oxidation), the other being photolysis: the process of being broken apart by photons ([33, 191, 101, 85]). These reactions lead to a daytime lifetime of a few hours ([10, 123]). Both these loss processes (photolysis, oxidation) form CO and hydroperoxyl radicals (HO_2), and have global significance to radiative forcing and oxidative capacity ([53]). The other notable sinks are wet and dry deposition, although these are not as significant ([10]) (TODO: add more cites here).

1.4.2 Measurement techniques

There are a few ways to measure HCHO, including Fourier Transform Infra-Red Spectrometry (FTIR) and Differential Optical Absorption Spectroscopy (DOAS). The DOAS technique takes advantage of the optically thin nature of HCHO in order to linearise the radiance differential through air masses with and without HCHO, using the Beer-Lambert intensity law. This method works for both in the home HCHO detection and global measurements from in-situ and remote sensing instruments ([66, 62, 37]). As a trace gas HCHO interferes with light over a few wavelength bands, which allows instruments to detect concentrations between a known light source and a detector. Figure 1.4 shows the interference spectrum of HCHO as well as a typical band used to examine interference in the DOAS technique. One difficulty is that this interference is relatively small (HCHO is optically thin) and other compounds absorb light at similar wavelengths ([37]). FTIR measurements can have a range of uncertainties, including systematic and random measurement errors and uncertain apriori shape factors and water profiles (eg: [53]).

DOAS

TODO: some of this is repeated in isoprene chapter satellite section. The DOAS technique uses solar radiation absorption spectra to measure trace gases through paths of light. Beer's law states that $T = I/I_0 = e^{-\tau}$ with T being transmittance, τ being optical depth, and I, I_0 being radiant flux received at instrument and emitted at source respectively. From $\tau_i = \int \rho_i \beta_i ds$ we get:

$$I = I_0 \exp \left(\sum_i \int \rho_i \beta_i ds \right)$$

Where i represents a chemical species index, ρ is a species density (molecules per cm^3), β is the scattering and absorption cross section area (cm^2), and the integral over ds represents integration over the path from light source to instrument.

Multiple axis DOAS (MAX-DOAS) uses DOAS over several open path directions and also examines the infra-red light interference. In [53], an FTIR spectrometer at Jungfraujoch is compared against both MAX-DOAS and satellite data, with two CTMs; GEOS-Chem and IMAGES v2 used to compare total columns and vertical resolution of each instrument. Generally satellites use a DOAS based technique, with chemical transport and radiative transfer models used to transform the non-vertical light path interference into vertical column amounts.

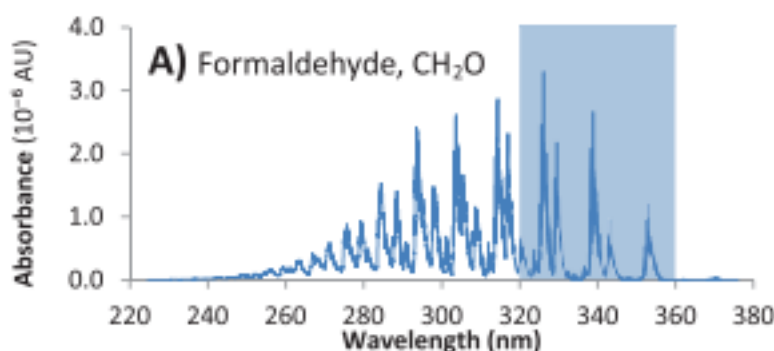


FIGURE 1.4: HCHO spectrum, with a typical band of wavelengths used for DOAS path measurements. This is a portion of an image from [37].

MAX-DOAS is a remote sensing technique which uses several DOAS measurements over different viewing paths. In these retrievals, the measurements of light absorption are performed over several elevations in order to add some vertical resolution to the measurement of trace gas concentrations. An example of this is shown in figure 1.5, which was taken from [95]. Recently MAX-DOAS has been used to examine HCHO profiles in the clean free troposphere ([53, 157]) as well as in polluted city air ([95]). Depending on orography and atmospheric composition (ie. the influence of interfering chemicals), MAX-DOAS can be used to split the tropospheric column into two partial columns; giving a small amount of vertical resolution to HCHO measurements [53, 95, eg.].

DOAS methods are based on light interference and absorption through air masses. Other types of measurement involve directly measuring the air, and determining chemical compounds through their physical properties. A proton transfer reaction mass spectrometer (PTR-MS) can be used to determine gas phase evolution of terpene oxidation products ([Lee2006a, Nguyen2014, 199, eg.]). This is done through analysis of mass to charge ratios (m/z) of ionised air masses which are then identified as chemical compounds. [Nguyen2014] use and compare several instruments (including one which is PTR-MS based) in the analysis of isoprene and monoterpene products. A Gas Chromatography mass spectrometer (GC-MS) is also able to identify isoprene, monoterpenes, and their products [Nguyen2014].

Other measurement techniques include chromatographic and fluorimetric methods, both of which differ widely from each other and the spectroscopic methods ([68]). [68] examine a single air mass with 8 instruments using the four techniques (MAX-DOAS, FTIR, chromatographic, and fluorimetric), and show that reasonable agreements can be achieved. Generally the measurements were somewhat close, the five Hantzsch instruments agreeing to within 11% (after removing two potentially faulty measurements), although different calibration standards were used. Titration for the different calibration solutions could not be resolved, which may account for absolute offsets up to 30%. These differences and non-uniformities between measurements (even among identical instruments) are part of the reason HCHO does not have a consistent network for global measurements like those for GHGs or Ozone ([27]).

In-situ measurements also contain errors, depending on the device used and chemical being measured this error can be significant. [43] analyse the uncertainty of VOC

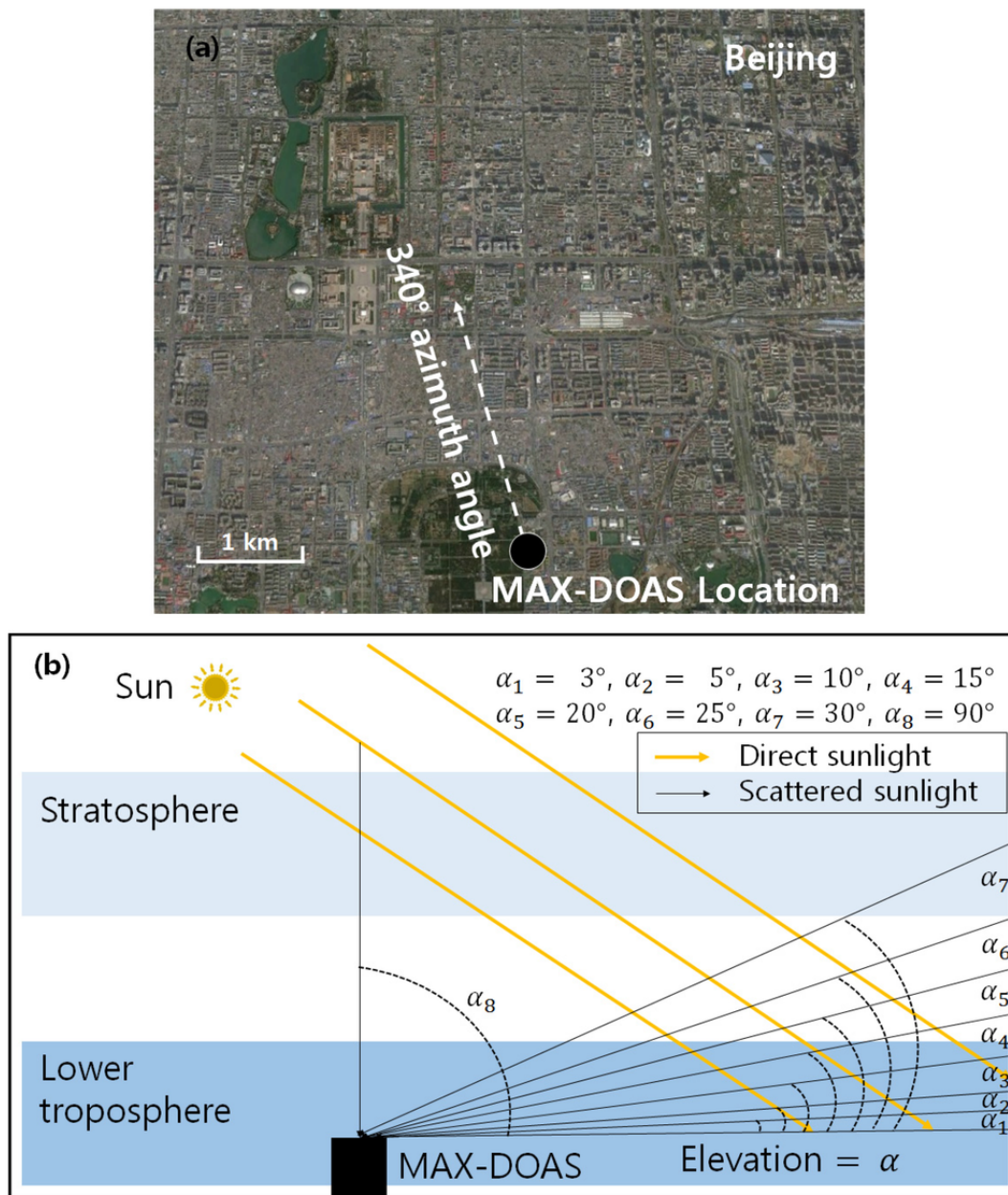


FIGURE 1.5: Image from [95].

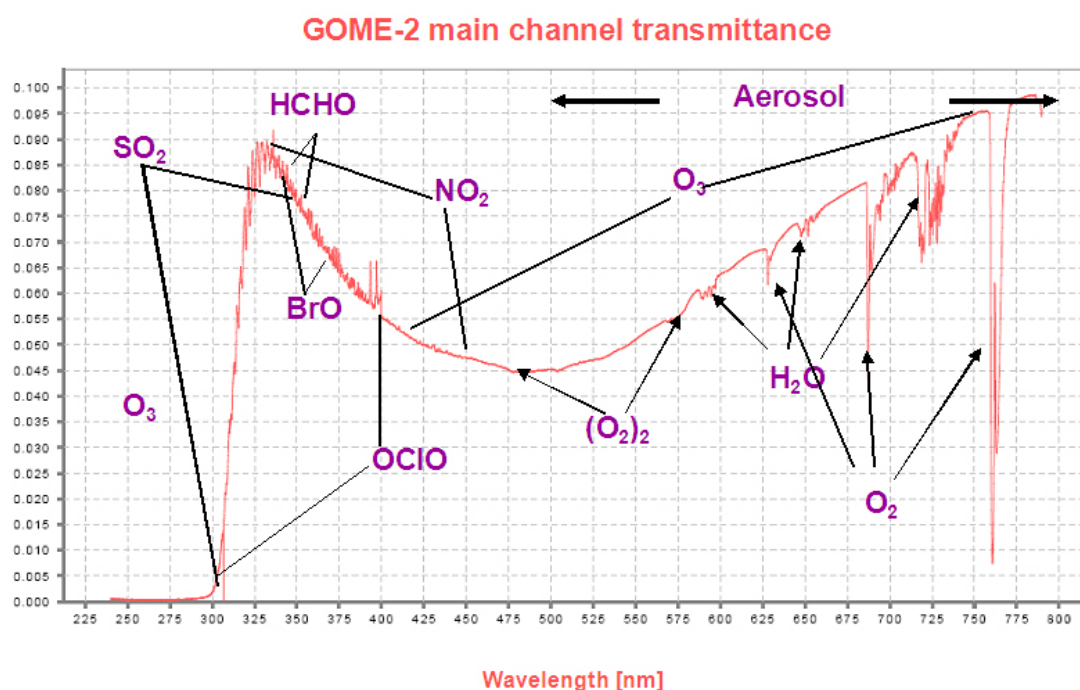


FIGURE 1.6: An example spectrum showing interferences used for species concentration measurements by GOME-2. Image by EUMETSAT and ESA ([50].

)

measurements (including isoprene) using three different techniques during a campaign in Sydney in 2012. The major sources of uncertainty in measurement techniques included interference from non-target compounds and under-reporting. Overall isoprene uncertainty in their measurements was a factor of 1.5 to 2. This can feed into uncertainties in modelling and satellite retrievals, as verification and correlations are affected.

Satellite measurements

Several satellites provide long term trace gas observations with near complete global coverage, including the ERS-2 launched in April 1995 which houses the GOME ultraviolet and visible (UV-Vis) spectrometer, the AURA launched in July 2004 which houses the OMI UV-Vis spectrometer, the MetOp-A and B launched in October 2006 and September 2012 respectively both housing a GOME-2 UV-Vis spectrometer. These satellites are on Low Earth Orbit (LEO) trajectories and overpass any area up to once per day. Satellites can use DOAS techniques with radiative transfer calculations on solar radiation absorption spectra to measure column HCHO. An example of a spectrum retrieved from the GOME-2 instrument is given in figure 1.6.

Measurements done using DOAS often apply a forward radiative transfer model (RTM) such as LIDORT in order to determine a trace gas's radiative properties at various altitudes. The forward RTM used for satellite data products also involves functions representing extinction from Mie and Rayleigh scattering, and the efficiency of

these on intensities from the trace gas under inspection, as well as accounting for various atmospheric parameters which may or may not be estimated (e.g. albedo).

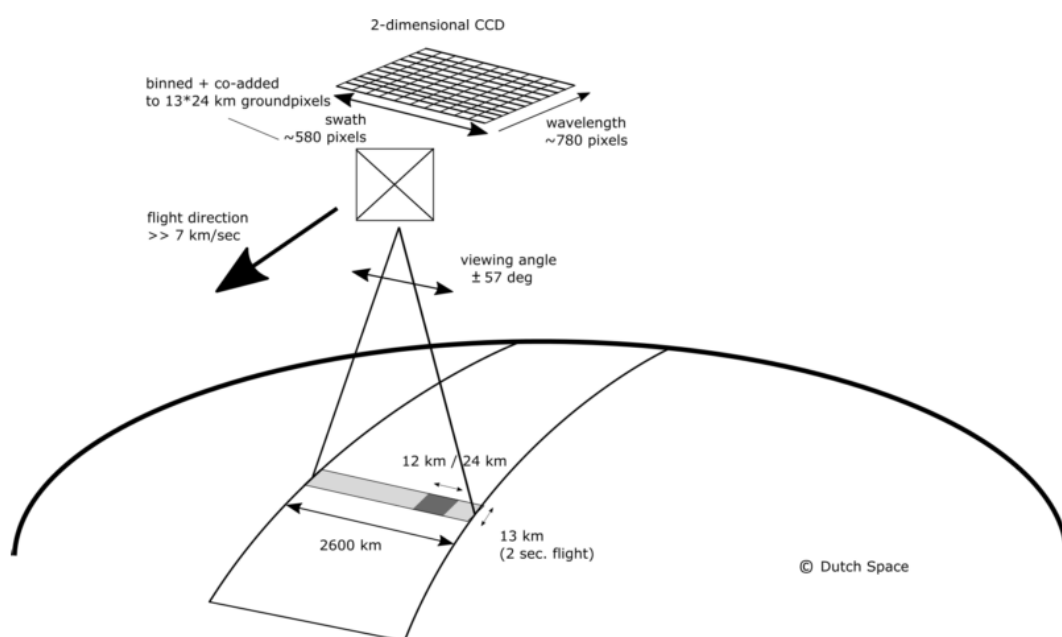
Satellites record near nadir (vertical) reflected spectra between around 250-700 nm split into spectral components at around 0.3 nm in order to calculate trace gases including O₃, NO₂, and HCHO (eg: [100]). Several public data servers are available which include products from satellites, including NASAs Earthdata portal (<https://earthdata.nasa.gov/>) and the Belgian Institute for Space Aeronomy (IASB-BIRA) Aeronomie site (<http://h2co.aeronomie.be/>).

Satellite measurements are generally performed using spectral fitting followed by conversion to vertical column densities. The use of multiple satellites can even be used to detect intradiel concentrations in trace gas columns, as shown in [171] using OMI and GOME-2 measurements, which have respective overpass times of 1330 and 0930 LT. Instruments including MODIS on board the AQUA and TERRA satellites are also able to determine aerosol optical depth (AOD), a measure of atmospheric scatter and absorbance. An AOD of under 0.05 indicates a clear sky, while values of 1 or greater indicate increasingly hazy conditions. This is important in order to determine where measurements from other instruments may be compromised by high interference. Satellite measured AOD requires validation by more accurate ground based instruments like those of AERONET which uses more than 200 sun photometers scattered globally.

Soon even more HCHO data will be available in the form of geostationary satellite measurements ([90]). [90] examine simulated geostationary measurements against GEOS-Chem column simulations to determine the most important instrument sensitivities. Geostationary satellites can provide temporally rich measurements over an area, as they are not sweeping around the earth but fixed relative to one latitude and longitude.

OMI

The OMI instrument on board AURA has been active since July 2005, it records spectra from 264-504 nm using an array of 60 detectors with mid-resolution (0.4-0.6 nm). This band of wavelengths allows measurements of trace gases including O₃, NO₂, SO₂, HCHO, and various other quantities like surface UV radiation. Recently [156] analysed the performance over time of the instrument and found irradiance degradation of 3-8%, changed radiances of 1-2%, and a stable wavelength calibration within 0.005-0.020 nm. They also provide a very nice summary of the OMI instrument copied here in Fig. ??, as it shows the instruments spectral, temporal, and spatial resolutions. These changes are measured excluding the row anomaly (RA) effect, which is relatively stable since 2011, although it is still growing and remains the most serious concern. An analysis of the row anomaly by [75] state that OMI ozone columns remain suitable for scientific use, with recommendation for further evaluation. And analysis of OMI output by [156] concludes that data is still of high quality and will deliver useful information for 5-10 more years, with radiances only changing by 1 – 2% outside of RA impacted areas. The RA began in June 2007, with some cross-track rows seemingly blocked. The most likely cause is some instrument insulation partially obscuring the radiance port ([156]).



Channel	Wavelength range	Spectral resolution	Spectral sampling	Ground pixel size
UV1	264–311 nm	0.63 nm = 1.9 px	0.33 nm px ⁻¹	13 × 48 km
UV2	307–383 nm	0.42 nm = 3.0 px	0.14 nm px ⁻¹	13 × 24 km
VIS	349–504 nm	0.63 nm = 3.0 px	0.21 nm px ⁻¹	13 × 24 km

AMF

To convert the trace gas profile from a reflected solar radiance column (slanted along the light path) into a purely vertical column requires calculations of an air mass factor (AMF). In satellite data, the AMF is typically a scalar value for each horizontal grid point which will equal the ratio of the total vertical column density to the total slant column density. This value requires calculations to account for instrument sensitivities to various wavelengths over resolved altitudes, and is unique for each trace gas under consideration.

An AMF characterises measurement sensitivity to a trace gas at various altitudes [140, e.g.]. [109] show that AMF calculations can be the largest source of uncertainty in satellite measurements. Another way of describing AMFs are as measures of how radiance at the top of the atmosphere (TOA) changes with trace gas optical depths at specific altitudes ([109]). Calculation of the AMF is important as it is multiplied against the estimated slant columns in order to give vertical column amounts.

Related to the AMF is the averaging kernel (AK), which is used to handle instrument measurements which are sensitive to concentrations at different altitudes in the atmosphere. DOAS methods can be heavily influenced by the initial estimates of a trace gas profile (the *a priori*) which is often produced by modelling, so when comparing models of these trace gases to satellite measurements extra care needs to be taken to avoid introducing bias from differing *a priori* assumptions. One way to remove these *a priori* influences is through the satellites AK (or by using AMFs), which takes into account the vertical profile of the modelled trace gas and instrument sensitivity to the trace gas ([49, 140]). [91] recommends that when comparing satellite data to models, the AMF should first be recalculated using the model as an *a priori*. This is in order to remove any *a priori* bias between model and satellite columns.

Uncertainties

While satellite data is effective at covering huge areas (the entire earth) it only exists at a particular time of day, is subject to cloud cover, and generally does not have fine horizontal or vertical resolution. Concentrations retrieved by satellites have large uncertainties, which arise in the process of transforming spectra to total column measurements, as well as instrument degradation (satellite instruments are hard to tinker with once they are launched). Uncertainty in transforming satellite spectra comes from a range of things, including measurement difficulties introduced by clouds, and instrument sensitivity to particular aerosols [123]. Many products require analysis of cloud and aerosol properties in order to estimate concentration or total column amounts [140, 139, 112, 188]. The main source of error in satellite retrievals of HCHO are due to instrument detection sensitivities, and the vertical multiplication factor (discussed in more detail in Section 4.7.2) [123].

There are two types of measurement error, arguably the worst of these is systematic error (or bias) which normally indicates a problem in calculation or instrumentation. If the systematic error is known, it can be corrected for by either offsetting data in the opposite direction, or else fixing the cause. A proper fix can only be performed if the sources of error are known and there is a way of correcting or bypassing it. Random

error is the other type (often reported as some function of a datasets variance, or uncertainty), and this can be reduced through averaging either spatially or temporally. By taking the average of several measurements, any random error can be reduced by a factor of one over the square root of the number of measurements. This is done frequently for satellite measurements of trace gases (which are often near to the detection limit over much of the globe). For example: [190] reduce the measurement uncertainty (in SCIAMACHY HCHO columns) by at least a factor of 4 through averaging daily over roughly 500km around Saint-Denis, and only using days with at least 20 good measurements.

Satellite measurements of HCHO are relatively uncertain, however this can be improved by averaging over larger grid boxes or longer time scales. An example of this can be seen in [42], where monthly averaging is used to decrease the measurements uncertainty. They examine HCHO in Europe, which is low; near the detection limit of satellite measurements. Taking monthly averages allows enough certainty that useful inversions can be determined to estimate the source emissions of HCHO. The finer nadir resolution of OMI (13 by 24 km²) compared to other satellites reduces cloud influence ([123, 124]). Although the uncertainty in each pixel is $\sim 2 \times 10^{16}$, which is $5 \times$ higher than GOME, there are $\sim 100 - 200 \times$ as many measurements due to the smaller footprint and better temporal resolution of OMI, which allows a greater reduction of uncertainty with averaging ([76, 124]).

In cloudy, hazy or polluted areas measurements are more difficult to analyse ([e.g. 139, 113]). Recent work by [188] showed that updating how the surface reflectivity is incorporated into satellite measurements can change the retrievals by 50 % in polluted areas.

In satellite HCHO products, concentrations over the remote pacific ocean are sometimes used to analyse faulty instrument readings. This is due to the expected invariance of HCHO over this region. For instance GOME (an instrument which measures trace gases on board the ERS-2) corrects for an instrument artifact using modelled HCHO over the remote pacific ([Shim2015]). OMI HCHO products use a similar technique to account for sensor plate drift and changing bromine sensitivity ([62])

For many places the tropospheric column HCHO measured by satellite is biased low, [209] examine six available datasets and show a bias of 20 - 51% over south east USA when compared against a campaign of aircraft observations (SEAC⁴RS). [40] also found a low bias from 20 - 40% when comparing OMI and GOME2 observations against ground based vertical profiles, and [16] determine OMI to be 37% low compared with aircraft measurements over Guyana. These bias can be corrected by improving the assumed apriori HCHO profiles which are used to calculate the AMFs of the satellite columns. [123] examine OMI HCHO columns over North America and determine overall uncertainty to be 40%, with most of this coming from cloud interference. [124] shows that there also exists some latitude based bias, as well as a systematic offset between the OMI and GOME instruments. This does not appear to be due to the different overpass times of the two instruments.

Uncertainty in the OMI satellite instrument is calculated by the Smithsonian Astrophysical Observatory (SAO) group using the uncertainty in backscattered radiation retrievals ([62, 1]). Another method of calculating the uncertainty is used by the Belgian Institute for Space Aeronomy (BIRA) group, who determine uncertainty from the

standard deviation of HCHO over the remote pacific ocean [39, 40].

A full analysis of the AMF uncertainty in OMI measurements, as well as the structural uncertainty (between different systems of calculations applied to the same data) is performed by [109]. They determine the structural uncertainty using ensemble techniques on seven AMF calculation approaches used by different retrieval groups. They show that in scenarios where the gas is enhanced in the lower troposphere, AMF calculation is the largest uncertainty in satellite measurements. In polluted environments the structural uncertainty is estimated at 42 %, or 31 % over unpolluted environments. The importance of apriori and ancillary data (such as surface albedo and cloud top height) is also shown, as it sharply affects the structural uncertainty.

GOME suffers from similar uncertainties to OMI, as the same general method of DOAS remote measurements are performed. The uncertainty from slant column fitting has been calculated for GOME to be 4×10^{15} molecules cm^{-2} [25, 123]. The conversion factor for slant to vertical columns (AMF) calculation also suffers from errors; primarily from surface albedo, HCHO vertical profile apriori, aerosol, and cloud influence [123]. AMF uncertainties for GOME are calculated to be 1 to 1.3×10^{15} molecules cm^{-2} by [159].

In conjunction with atmospheric chemistry and radiative models, satellite measurements can be used to quantify the abundance of several chemical species in the atmosphere. Isoprene is hard to measure directly due to its short lifetime and weak spectral absorption, instead HCHO is often used as a proxy ([123, 55, 42, 112, 17, 85, 18]). This leads to a method of isoprene emissions estimation termed top-down (as opposed to bottom-up estimates like MEGAN). The existence of satellite data covering remote areas provides an opportunity to improve VOC emissions estimates leading to more robust models of global climate and chemistry. Satellite data allows us to verify large scale models of natural emissions, and their subsequent chemistry.

1.4.3 Glyoxyl TODO: move somewhere fitting?

Another chemical retrievable from satellite observation is Glyoxyl, which can be used to further determine what sort of precursors to HCHO are being emitted [169, 121, 122]. TODO: go through 2014 paper and see if it's easy to retrieve, then email Dr. Chris Miller. For example [Cao2018_discuss] recently used Glyoxyl measurements to improve understanding of biogenic and anthropogenic NMVOC emissions over China. This involved using a method pioneered by [169] TODO: get this cite and check method out.

Glyoxyl (CHOCHO) is important to us as it shares many properties with HCHO, and may provide additional information in determining isoprene emissions. Glyoxyl is another product of VOC oxidation in the atmosphere, with isoprene being the main source globally. Under high NO_x conditions, glyoxyl forms rapidly, similarly to HCHO. However, glyoxyl also forms in low NO_x environments both slowly (through isoprene epoxydiols), and rapidly (through di-hydroperoxide dicarbonyl compound photolysation [32]). This process is similar to the proposed mechanisms for hydroperoxyaldehydes by [83] and carbonyl nitrates [127]. Aromatics which are largely anthropogenic form glyoxyl quickly, while HCHO is produced slower, allowing determination of anthropogenic sources [Cao2018_discuss].

HCHO has been used to estimate isoprene emissions (some examples in Section ??) but many uncertainties exist. One of these uncertainties is the yield of HCHO from isoprene, especially in low NO_x environments. Glyoxyl could prove complementary to HCHO in constraining isoprene emissions (TODO: Read and cite Vrekoussis2009,2010, Chan Miller 2014, Alvarado 2014) [122]. Recently [122] updated GEOS-Chem to include the prompt formation of glyoxyl and compared this with satellite and airplane measurements over the USA. With coming geostationary satellites, which provide greater time resolved measurements of HCHO and CHOCHO, this mechanism could be used to clearly show when low NO_x isoprene chemistry is being undertaken [122].

1.5 Modelling

Models can fill the gaps (both spatial and temporal) in measurement records, and are used to predict/avoid/mitigate hazardous scenarios. They are used ideally to steer us away from unsustainable pollution and help complete our understanding of the world from small to large scales. They can be used to increase measurement accuracy (for instance in satellite measurements) and determine where we lack information, while also checking the performance of new instruments. Precisely representing various chemicals and reactions in the atmosphere allows efficient mitigation of pollution, since we can compare scenarios against one another. Currently, improved isoprene understanding is critical for effective air quality measuring [Marvin2017].

Atmospheric chemical models provide a simulation of chemical densities and transport over time, through the atmosphere. They require various inputs in order to accurately represent scenarios or regions on earth. Models of emissions are often used as drivers for atmospheric chemistry models, which generally require initial and boundary conditions in order to run.

1.5.1 Chemistry

Chemical Transport Models (CTMs) simulate production, loss, and transport of chemical species. This is generally calculated using one or both of the Eulerian (box) or Lagrangian (puff) frames of reference. CTMs normally solve the continuity equations simultaneously with chemical production and loss for chemicals under inspection. The continuity equations describe transport of a conserved quantity such as mass, which, solved together with production and loss of a chemical can provide detailed simulations of natural processes.

The general continuity equation links a quantity of a substance (q) to the field in which it flows and can be described by the formula:

$$\frac{\partial \rho}{\partial t} + \nabla \cdot j = \sigma$$

where ρ is density of q in the field, t is time, ∇ is divergence, j is the flux (q per unit area per unit time entering or leaving the field), and σ is the generation or loss of q per unit volume per unit time.

The type of model best suited to modelling the entire earth uses the Eulerian frame of reference, where the atmosphere is broken up into 3-D boxes with densities and

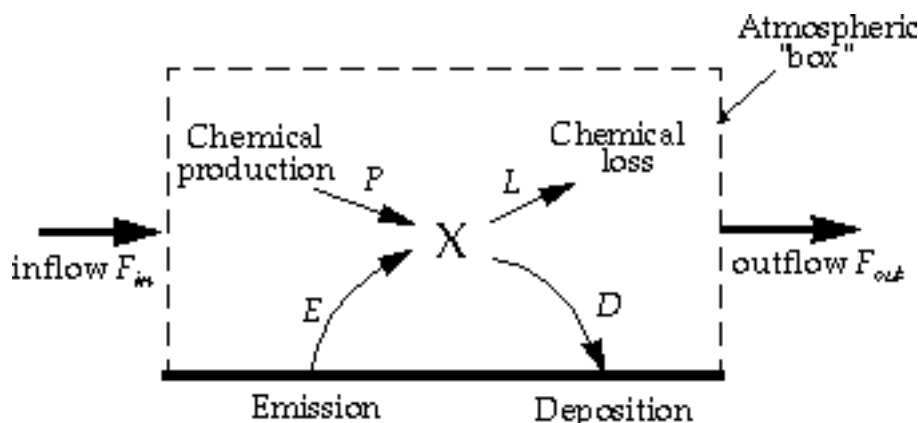


FIGURE 1.7: Standard box model parameters, image taken from [78].

transport calculated and stored for sequential steps in time at each location. The mass balance equation must be satisfied in any realistic long term box model and is as follows:

$$\begin{aligned} \frac{dm}{dt} &= \sum \text{sources} - \sum \text{sinks} \\ &= F_{in} + E + P - F_{out} - L - D \end{aligned}$$

where m is mass of a chemical, E and D are emission and deposition, P and L are production and loss, and F is chemical transport in and out, as shown in figure 1.7. Many chemical species interact with each other through production and loss. Any large chemical model will solve this mass balance equation over highly coupled arrays of partial differential equations which can be complex and time consuming.

In many CTMs the isoprene emissions are calculated separately using MEGAN, and then used as boundary conditions (EG: [63]). This can speed up calculations as the transport and concentrations can be simulated in various conditions without recalculating the emissions. Trace gases with short lifetimes and complex chemistry such as isoprene are often hard to measure which makes verifying model estimates difficult.

Contemporary models generally use mathematical differential solving tools of various complexity to solve chemical equations and reaction rates (often called chemical mechanisms) in order to predict an environments evolution over time. Different solvers may be slower or faster and more suited to particular situations based on the stability of the equations and systems involved, and chemical mechanisms may vary in how many reactions and chemicals are listed and grouped together. For example: Since $[O] \ll [O_3]$ the chemical family O_X ($O_X \equiv O + O_3$) can be used to simplify chemistry simulations and approximate O_3 concentrations [BrasseurJacob2017]. [206] examine the outputs from a regional model (WRF/Chem) using three different chemical mechanisms, and they show that particulate matter prediction is sensitive to the choice of chemical mechanism.

GEOS-Chem

GEOS-Chem is an example of this, with many boxes covering the globe, each with chemistry and dynamic meteorological conditions. Different meteorological conditions such as wind and air pressure need to be handled within each box. GEOS-Chem has a meteorological model coupled to a chemical model, which simulates the world in a three dimensional grid of connected boxes.

GEOS-Chem is a well supported global, Eulerian CTM with a state of the science chemical mechanism, with transport driven by meteorological input from the Goddard Earth Observing System (GEOS) of the NASA Global Modeling and Assimilation Office (GMAO). GEOS-Chem simulates more than 100 chemical species from the earth's surface up to the edge of space (0.01 hPa) and can be used in combination with remote and in-situ sensing data to give a verifiable estimate of atmospheric gases and aerosols. It was developed, and is maintained, by Harvard University staff as well as users and researchers worldwide. Several driving meteorological fields exist with different resolutions, the finest at 0.25 by 0.3125° horizontally at 5 minute time steps with 72 vertical levels.

Global CTMs are often run using one or several emission models (or the output from them) to determine boundary conditions for many gridboxes. TODO: is this the case? Doesn't GEOS-Chem have coupled chemistry and meteorology? Check the wiki. GEOS-Chem has boundary conditions based on several meteorological and emissions inventories, the following are the versions of theses used by GEOS-Chem v 10.01. Meteorological fields can be driven by NASA's GEOS-5 data (0.5° × 0.666°) [26], which exists up to 2013, or GEOS-FP data (0.25° × 0.3125°). Fire emissions come from the GFED4 product [59]. Anthropogenic VOC emissions come from the EDGAR inventory, while biogenic VOC emissions are coupled to the MEGAN model TODO:cites. The estimated biogenic VOC emissions are important for accurately simulating chemistry within models, as discussed in Sections ?? and 1.5.4.

Box models

Box models are much smaller scale than global CTMs, examining one uniform environment with many parametrisations such as transport and emissions. Box models can be used to check chemical mechanisms in specific scenarios, such as high or low NO_x environments. [Marvin2017] use a box model matching conditions in southeast USA to evaluate isoprene mechanisms from several models. A box model involves modelling chemistry in a singular set of conditions without transport or any spatial gradients. One box model used in this thesis is called CAABA/MECCA, and is described in Section 2.3.

By allowing for interactions between boxes this concept can be extended to multiple-box models. These are simply multiple instances of single boxes with the addition of transport between them, which generally requires a meteorological model to provide winds, and other transport mechanisms.

1.5.2 Emissions

There are two commonly used ways of estimating isoprene emissions, top-down or bottom-up. Bottom-up emission estimates generally model the flora and events which emit isoprene, like Eucalypts, factories, shrubs, etc. They use various properties of the emitters in order to estimate how much isoprene is being produced. Some of these properties include leaf areas, speciated responses to sunlight and temperature, moisture stress, etc ([66, 63]). Understanding how much isoprene is emitted, when and by what, is complicated. Since little data exists with which to verify many of these bottom-up emission inventories, they can be uncertain on a large scale. Emissions inventories such as MEGAN are bottom-up and use models of emissions based on tree types, weather, and other parameters.

[170] examined modelled Asian emissions and altered model parameters for temperature, plant type emission factors, incoming solar radiation (insolation) intensity, land use changes, and palm tree forest expansion. Changes were constrained by a network of radiation measurements and some experiments with south east Asian forest emissions - and led to reduction in isoprene emissions by a factor of two over the region. The Asian region is also shown to have a strong correlation with the Oceanic Niño Index (ONI), with positive anomalies associated with El Niño. In the last 20 years anthropogenic emissions of VOCs have been increasing while biogenic VOC emissions have decreased due to rapid economic growth and lower annual temperatures [170, 90].

MEGAN

MEGAN is a global model with resolution of around 1 km, and is used to generate the BVOC emissions used in various global chemistry models such as GEOS-Chem. MEGAN uses leaf area index, global meteorological data, and plant functional types (PFTs) to simulate terrestrial isoprene emissions. The model includes global measurements of leaf area index, plant functional type, and photosynthetic photon flux density, from remote sensing databases [85]. The various PFTs are used to generate emission factors which represent quantities of a compound released to the atmosphere through an associated activity. For example, an emission factor for isoprene within a forest would include the requirement of sunshine and suitable temperature. The schematic for MEGAN, taken from Guenther [65], is shown in figure 1.8

MEGAN “is a modelling framework for estimating fluxes of biogenic compounds between terrestrial ecosystems and the atmosphere to account for the major known processes controlling biogenic emissions.” [64]. It allows parameterisation of various BVOC emissions, with descriptions given in [64]. Instructions to run version 2.1 are available at http://lar.wsu.edu/megan/docs/MEGAN2.1_User_GuideWSU.pdf, and a version using the Community Land Model (CLM) is available at <http://www.cesm.ucar.edu>. It uses meteorological fields from the Weather Research and Forecasting (WRF) modelling system. Version 2.1 (updated from 2.0 [63]) includes 147 species, in 19 BVOC classes, which can be lumped together to provide appropriate output for mechanisms in various chemical models.

MEGAN was developed as a replacement for two earlier canopy-environment emission models (BIES and GEIA), and initially included a simple canopy radiative

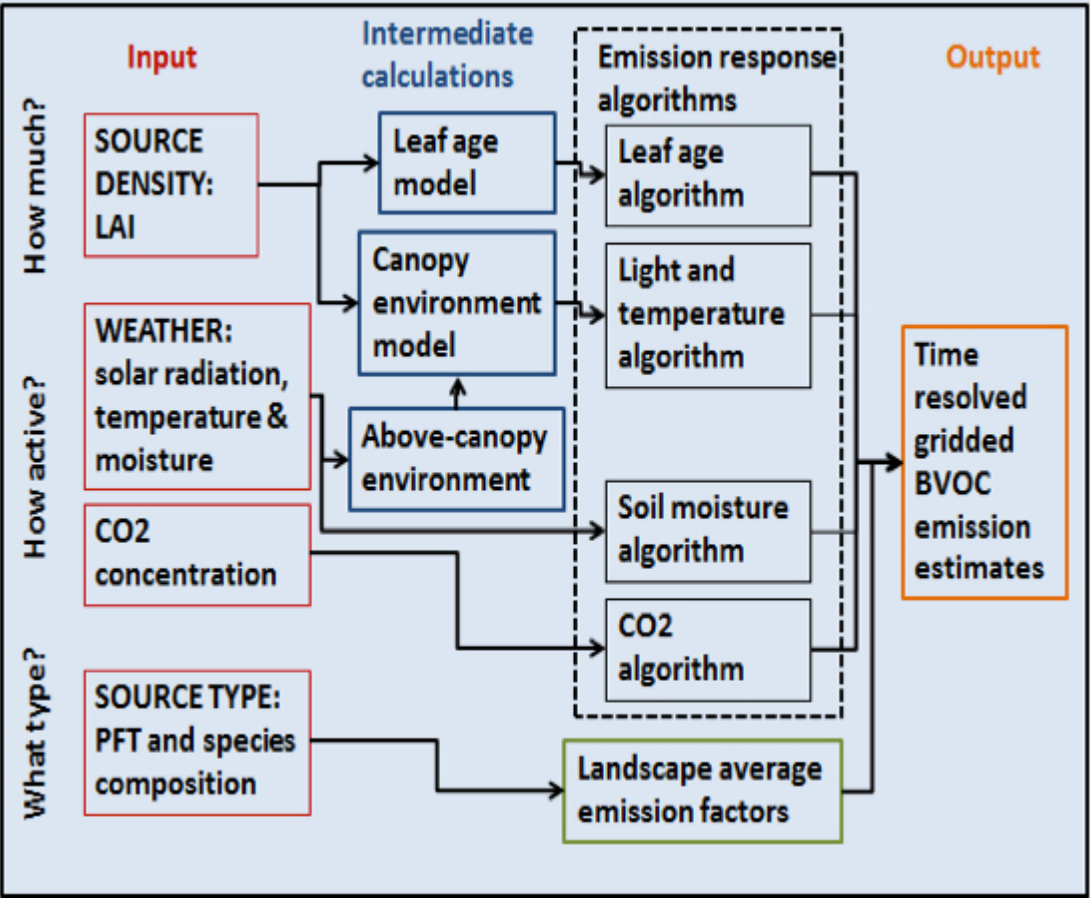


FIGURE 1.8: MEGAN schematic, copied from Guenther [65]

transfer model, which parameterised sun-lit and shaded conditions through a canopy. Early models didn't account for abiotic stresses, such as drought, prior rainfall and development processes, although these influenced species specific emissions by more than an order of magnitude [133]. Isoprene emissions were based on temperature, leaf area, and light, but have since been updated to include leaf age activity [67], and a leaf energy balance model [63] in MEGANv2.0. This update included a parameter for soil moisture, to account for drought conditions, however this parameter is currently (as of version 2.1) not applied to isoprene [161]. Soil moisture effects on isoprene emission are very important, and can drastically affect estimates.

MEGAN has recently been analysed using 30 years of meteorological reanalysis information by [161]. They estimate emissions of Biogenic VOCs (BVOCs) to be 760 Tg(C)yr^{-1} , 70% (532 Tg(C)yr^{-1}) of which is isoprene. This is similar to isoprene emission estimates from MEGAN itself, of $400\text{--}600 \text{ Tg(C)yr}^{-1}$ [63]. MEGAN emissions estimates are termed bottom-up, as opposed to top-down which are derived from satellite measurements of the products of various VOCs. Using GOME satellite HCHO and a Bayesian inversion technique to derive isoprene emissions, [159] estimated global isoprene emissions to be $\sim 566 \text{ TgC yr}^{-1}$. This estimate is greater than initially thought and leads to decreased ($\sim 10\%$) simulated OH concentrations to $9.5\text{e}5 \text{ molec cm}^{-3}$.

[113] examine factors affecting isoprene emissions, showing how emissions are sensitive to various environmental factors. Their work used MEGAN [66] and GEOS-Chem to look at how these factors affect surface ozone and particulate matter in Africa. One of the important uncertainties seen in MEGAN within this work is the isoprene emissions due to plant type. Canopy level isoprene measurements are made using relaxed eddy accumulation (REA) at several sites in Africa. One plant type near a measurement site emits more than other species and its actual distribution on a larger scale is completely unknown - leading to possible overestimations in MEGAN. Current emissions estimates require more validation against observations, and recently a comparison of two major VOC models (MEGAN and ORCHIDEE) was undertaken by [119] reiterating this requirement. In their work they examine model sensitivities and show that the important parameters are leaf area index (LAI), emission factors (EF), plant functional type (PFT), and light density fraction (LDF). There is high uncertainty in LAI and EF, which require more or improved measurements at the global scale. LDF parameterisation needs improvement and these models require more PFTs. Global emissions inventories like MEGAN suffer from large extrapolations which introduce uncertainties [121].

1.5.3 Satellite inversion

Top-down estimates look at how much of a chemical is in the atmosphere and try to work out how much of its major precursors were emitted. This generally takes advantage of longer lived products which may reach a measurable equilibrium in the atmosphere. For isoprene this is done by looking at atmospheric HCHO enhancement, which can be largely attributed to isoprene emissions once transport and other factors are accounted for. Recently [171] used satellite HCHO measurements to constrain anthropogenic sources of isoprene and found good global agreement with the bottom up estimates, although some regions had sources differ by up to 25-40%. Their study

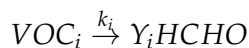
used the RETRO 2000 database for anthropogenic emission aprioris except for Asia in 2008 where REASv2 was used. Since 1997, when GOME first measured HCHO over Asia [181], satellites have been able to provide a total column measurement of HCHO, one of the primary products of isoprene.

Satellites recording reflected solar spectra use DOAS to measure various trace gases in the atmosphere, including formaldehyde. While satellite measurements can only be used during daytime hours, HCHO lifetimes are sufficiently short that any night-time chemistry will not affect midday observations [199]. Satellites can be used to measure the seasonal and interannual variability of HCHO over the globe. These records can be compared with modeled estimates of HCHO and used as a proxy to estimate isoprene emissions. This has been done in North America [139, 123], South America, Africa, China, Europe [42], and recently globally [27, 18]. Often these works use two forms of measurement such as satellite and aircraft data combined for validation ([113]). There is less information available from satellite measurements at higher latitudes due to increased errors ([40]).

Using HCHO to determine emissions of isoprene was initially performed by [140, 139], who used in-situ summertime HCHO measurements over North America as model validation. Isoprene emissions fluxes were derived using the Global Ozone Monitoring Experiment (GOME) satellite instrument. Palmer's method improved biogenic isoprene emissions estimates (compared with in-situ measurements) over two available inventories: the U.S. EPA Biogenic Emissions Inventory System (BEIS2) and the Global Emissions Inventory Activity (GEIA). This showed an inversion technique which could be used to improve large scale emissions estimates without further expensive measurement campaigns.

TODO: Read through this list of sources on the hcho to isop process : taken from Wolfe2015 Such techniques have informed isoprene emission inventories in North America (Abbot et al., 2003; Millet et al., 2008 ([139, 123, 141])), South America ([16]), 2008), Europe ([34, 42]), Africa ([112]), Asia (Fu et al., 2007; Stavrou et al., 2014), and globally (Fortems-Cheiney et al., 2012; ([159]); Stavrou et al., 2009).

Initially studies assumed a simple linear steady-state relationship between HCHO and it's precursors ([139, 141, 123]). This allowed a simple calculation of isoprene using the measured HCHO, with estimated reaction rates and yields. The methodology for calculating VOCs from HCHO is laid out in [139], and takes into account the expected lifetime and reaction rates of the precursor VOCs and HCHO. Assuming HCHO is produced quickly from short-lived intermediates, and the column is at steady state:



Where Y_i is HCHO yield per C atom (a measure of how much HCHO will form per gram of C from a VOC within a system), and k_i is the reaction rate. Then assuming a steady state of atmospheric HCHO (Ω molecules cm^{-2}) produced by oxidation of VOCs (VOC_i) and no horizontal transport:

$$\Omega = \frac{1}{k_{HCHO}} \sum_i Y_i E_i$$

Where i indexes a chemical species, k_{HCHO} is the HCHO loss rate due to OH and photolysis, Y_i is the molar HCHO yield from oxidation of i , and E_i is emission fluxes (C atoms $cm^{-2}s^{-1}$).

Estimates of Y_i can be attained from a model as shown in [123]. This involves a reduced major axis (RMA) correlation calculation between modelled HCHO and isoprene columns, multiplied by their loss rates (to photolysis and oxidation) (as a normalising factor). In high NO_x environments where HCHO has a lifetime on the order of 30 minutes, it can be used to map isoprene emissions with spatial resolution from 10-100 kms. Horizontal transport 'smears' the HCHO signal so that source location would need to be calculated using windspeeds and loss rates ([140, 139]). Smearing is explicitly handled in these studies due to the importance of transport and NO_x on forming robust and accurate estimates. Over Australia NO_x levels are generally not high enough to ensure quick HCHO formation and we must take extra care that we can account for the transport or 'smearing' caused by slower HCHO formation, details on this process can be found in Section 4.5.6.

Another method of correcting isoprene emissions using observed HCHO total column involves a Bayesian inversion. [159] work with GOME HCHO observations and GEOS-Chem, looking at areas with high signal to noise ratio (higher HCHO concentrations). They show that the model underestimates isoprene emissions and HCHO concentrations by 14-46%, with the corrected VOC emissions reducing the model biases to 3-25%.

The Bayesian inversion is also used in [34], where a regional CTM (CHIMERE) simulates HCHO, which is compared against OMI observed HCHO and shown to be regionally biased. This bias is expected to be caused by errors in MEGANs isoprene emissions estimations. The CHIMERE model is used to derive yields of HCHO from the various local VOCs and these are then used in estimating local emissions. The model is run initially with emissions of BVOCs and reactive anthropogenic VOCs (RAVOCs) turned off in order to work out the background (b) values of these compounds. The Bayesian inversion is used to correct regionally biased biogenic isoprene emissions by optimising these parameters in order to simulate HCHO closest to the observed HCHO levels. [34] uses CHIMERE as the forward model to determine the relationship between HCHO (y), isoprene and reactive anthropogenic VOCs (x), using

$$y = Kx + b + \epsilon \quad (1.3)$$

where ϵ are the (assumed) independent errors in measurements. K is the Jacobian matrix determined from CHIMERE representing the sensitivity of y to the state variable x . This K matrix is used in conjunction with error covariance in x to determine the Maximum A Posteriori (MAP) solution to calculate the optimal estimate of x (\hat{x}).

More recently, full inversions that better account for transport, source attribution, and chemical schemes have been implemented ([27]). TODO: full description of this better inversion technique going through FortemsCheiney2012.

[85] reviews remote sensing of BVOCs, which are on the rise, examining the last 20 years of data and analysis of the satellite products. Their review encompasses the latest reports up to 2014 The modelled isoprene and BVOC emissions from MEGAN

[67] of 500 and 1150 Tga⁻¹ respectively are still the global go to estimates. Their review reinforces the message that NMVOCs affect the oxidative capacity of the atmosphere and are largely driven by and sensitive to vegetation. The tropospheric affects from NMVOCs on the hydroxyl radical (OH), ozone (O₃), SOAs, and methane longevity, all interconnect to form a very complex system which still suffers from relatively large uncertainties in both measurement and chemistry mechanisms. One focus of [85] is HCHO, which is the dominant product of most BVOCs which is measurable by remote sensing. The main datasets of HCHO are from four satellite instruments: GOME on ERS-2, SCIAMACHY on ENVI-SAT, OMI on EOS AURA, and GOME2 on MetOp-A. These satellites have slightly different spectral and spatial resolutions, as well as using varied processes to estimate HCHO from detected radiances. This can lead to different estimates between instruments or methodologies as described in [Lorent2017], which means validation and comparison is more important when using these remotely sensed data.

Total HCHO is measured by satellite over the entire world, however the technique is not perfect and suffers from uncertainties and interferences. Satellite based chemical concentrations rely on ground-based measurements and modelled data for validation. They provide various readings with daily global coverage which is not otherwise feasible.

Validation is important due to the various uncertainties in the satellite remote sensing process, with apriori assumptions having the greatest effect on structural uncertainty between measurements techniques [109]. [209] use SEAC⁴RS aircraft HCHO measurements over the southeastern US as model validation, and show a bias in the assumed OMI shape factor that leads to a bias between satellite and SEAC⁴RS measurements. [113] compare OMI based isoprene emission estimates against relaxed eddy accumulation measurements from African field campaigns, as well as MEGAN and GEOS-5 inventories. [42] use HCHO from SCIAMACHY, and examine Europe using CHIMERE as the chemical model. In their work they show that satellite measurements can reduce source emission uncertainty by a factor of two, where emissions are relatively large.

1.5.4 Uncertainties?

Here I will attempt to list and partially explain the major uncertainties models have in relation to VOCs, SOAs, and ozone. TODO: Is this a good idea or should I put any pertinent uncertainties with the associated work/descriptions?

Emissions Inventories

Using different emissions inventories in an ACM can have large impacts on the simulation. Natural (biogenic or pyrogenic) and human driven (anthropogenic) emissions often drive a large fraction of atmospheric oxidation and radical chemistry, especially in the continental boundary layer. [204] examine the affects on CO and HCHO when running simulations with two different inventories. TODO: find where I took notes about Zeng2015 and put them here.

It is important to note that many estimates of isoprene emission are based on a few algorithms which can depend greatly on input parameters ([7, 134]). [7] argue that this

monopoly of emissions estimates may be leading us to an incorrect understanding of isoprene chemistry. [201] has shown that this is still a problem by looking at land carbon fluxes and modelling the sensitivity to VOC emissions estimates using two independent models of VOC emission. One model is photosynthesis based and estimates isoprene emissions using electron transfer energies and leaf physiology [133], while the other (MEGAN) uses the light and canopy temperature ([66, 8] TODO: Read Arneth et al., 2007; Unger et al., 2013). Both are sensitive to light and temperature parameterisations.

Improvements to emissions models require improved understanding of regions and their behaviour. Inaccuracies can arise due to lack of data, such as the large and sparsely measured Australian outback. MEGAN has been shown to overpredict isoprene and underpredict monoterpene emissions in southeast Australia, with peaks and troughs captured but not at the right magnitude ([48]). MEGAN output in Australia is adversely affected by poor emission factor estimation. An example can be seen in Müller et al. [128] where MEGAN overestimates isoprene in northern Australia. Underestimates of monoterpenes may be due simply to underestimated emission rates for many Eucalypt species [196].

Resolution

GEOS-Chem simulations are somewhat sensitive to the resolution at which you run. For example: [195] show that reduced resolution increases OH concentrations and ozone production rates. [28] find small changes in OH ($< 10\%$) in OH, HO₂ and ozone concentrations local to the north american arctic, when changing from 4 by 5 to 2 by 2.5 °resolution, however they continue at lower resolution to save computational time.

For many global scale analyses, errors from resolution are less important than those from chemistry, meteorology, and emissions ([28]). Many models lack in-situ measurements with which to verify their chemical mechanisms, leading to large discrepancies, as seen in [117]. TODO: briefly talk about Marvin2017a takeaways.

Chemistry mechanisms

There is still much work to be done in models to correctly simulate the various precursors to HCHO. Often HCHO is used as a way of checking if these precursors are correctly modelled since HCHO measurements are more readily available (for instance from satellites). GEOS-Chem has recently been analysed for sensitivity for ozone along with oxidants (OH and HO₂) [28]. [28] found that GEOS-Chem ozone was most sensitive to NO₂ photolysis, the NO₂ + OH reaction rate, and various emissions. They used GEOS-Chem v9-02, with $4^\circ \times 5^\circ$ resolution, and while the low resolution adds errors in OH concentrations and O₃ production rates, the errors from chemistry, meteorology, and emissions are much larger.

[Marvin2017] suggest that isoprene mechanisms in several contemporary models (including GEOS-Chem) are inadequate. They show that for a specific measurement campaign, the HCHO concentrations are underestimated in a way that can not be easily fixed through rate constant changes. Recently [Marvin2017] compared five global ACMS isoprene mechanisms by evaluating simulated HCHO mixing ratios

compared to in situ measurements from the Southeast Nexus (SENEX) aircraft campaign (in southeastern USA). They compared five models (GEOS-Chem, CB05, CB6r2, MCMv3.2, and MCMv3.3.1) and found all of them underestimated the HCHO concentrations (by 15 – 30%).

Another important factor in determining the yield of HCHO and other products from BVOCs is the local concentration of NO_x . [184] show how modelled surface ozone is overestimated due to high estimates of NO_x emissions, which affect oxidative capacity and VOC reactions.

Clouds

One of the major uncertainties in chemical, climate, radiation, and weather models is cloud formation and dynamics. Clouds are remarkably complex at a much finer scale than can be accurately modelled by global chemistry models (with current processing power). Globally over half (50-60%) of the world is covered by clouds, with $\sim 10\%$ of them being rain-clouds [84]. Wet scavenging performed in clouds not only depends on large scale cloud processes, but also on the microphysics of aerosols being scavenged, differing between aerosol sizes and hygroscopic properties. Isoprene emissions estimates are still fairly uncertain, as global measurements are difficult and regional emissions can be very different. The global uncertainty of isoprene emission was estimated to be a factor of 2 to 5 ($250\text{--}750 \text{ Tg yr}^{-1}$) [84]. Improvements over the years have been incremental, and generally localised to regions of particular interest for air quality such as China and the USA TODO: find recent uncertainty estimate improvements examples. The lack of accuracy in BVOC emissions estimates prevents accurate determinations of the sources and distribution of pollutants including ozone and organic aerosols. Most of the tropospheric SOA comes from biogenic precursors, the evidence for this has grown over the last two decades [66, 84, 64]. Accuracy in VOC measurements is important: it has been shown that even the diurnal pattern of isoprene emissions has an effect on modelling ground level ozone [70, 51].

Soil Moisture

Australia has a unique climate, along with soil moisture, clay content and other important properties which affect VOC emissions. These properties are poorly understood in Australia due to the continents size and the relative sparsity of population centres, which make many areas very difficult or expensive to reach. Soil moisture plays an important role in VOC emissions, as trees under stress may stop emitting various chemicals. This is especially true for Australia due to frequent droughts and wildfires. The argument for improved understanding of land surface properties, specifically soil moisture, is an old one[Chen2001, 125, 153]. [153] show how quickly soil moisture anomalies affect rainfall and other weather systems, while [Chen2001] specifically show how important fine scale soil moisture information is when modelling land surface heat flux, and energy balances. Modelled emissions are sensitive to soil moisture, especially near the soil moisture threshold (or wilting point), below which trees stop emitting isoprene and other VOCs completely as they can no longer draw water [18]. MEGAN accounts for soil moisture by applying it as an emission factor (EF) which scales the emission rate of various species. [161] show reductions in modelled

Australian isoprene emissions of 50% when incorporating soil moisture in MEGAN estimates.

Droughts affects can be difficult to measure, as it is a multi-scale problem which affects various aspects of the land-air interface including plant emissions and dry deposition ([192]). The Standardised Precipitation Evapotranspiration Index (SPEI) is a measure of drought using TODO [166]. This product covers 1901 - 2011, and uses the average over that period as the background, in order to compare drought stressed regions against those with sufficient or excess water [166].

1.6 Australia

In Australia most long term air quality or composition measurements are performed in or near large cities. Australia is dominated by areas with little anthropogenic influence and no ground based measurements of the natural emissions taking place [187]. Due to the lack of in-situ ground based measurements, estimates of VOC emissions are uncertain, with large scale extrapolation required [123]. Since many Australian cities are on the edge of regions with rich VOC emissions, it is very important to clarify the quantity, type, and cause of VOC emissions. Understanding of emissions from these areas is necessary to inform national policy on air pollution levels.

Biomass burning in southern Africa and South America has previously been shown to have a major influence on atmospheric composition in Australia [137, 61, 46], particularly from July to December [138, 106].

[63] estimated that the Australian outback is among the worlds strongest isoprene emitters with forests in SE Australia having emission factors greater than $16 \text{ mg m}^{-2} \text{ h}^{-1}$ (see figure 1.9). Measurement campaigns in SE Australia have since cast doubt on the emission factors used by MEGAN, as the Eucalyptus trees and soil moisture were poorly studied [48]. These emissions factor estimates are not well verified and measurements of isoprene (or other BVOC) emissions barely cover Australia either spatially or temporally. However, comprehensive coverage of one high yield product (HCHO) in the atmosphere over Australia exists in the form of satellite measurements.

1.6.1 VOCs

Bottom up inventories of VOCs remain largely uncertain due to extensive extrapolation over plant functional types, changing land cover, and parameterised environmental stressors [67, 84, 123]. VOC emission estimates are highly sensitive to many factors, several of which are not well characterised in Australia [161, 18]. Changes in parameterisation of soil moisture in the Model of Emissions of Gases and Aerosols from Nature (MEGAN, [66]) lead to massive changes in Australian isoprene emission estimates [161]. Over Australia MEGAN has problems involving unpublished plant functional types and their emissions, as well as poorly optimised soil moisture parameterisation [48].

Australia has the potential to be a major hotspot of isoprene emissions according to [63, 64], which shows heavy emissions factors in the region. Although recent work suggests that some Australian eucalypts may not be as egregious isoprene emitters as once thought [48]. Emissions in MEGAN are based on plant functional types, which

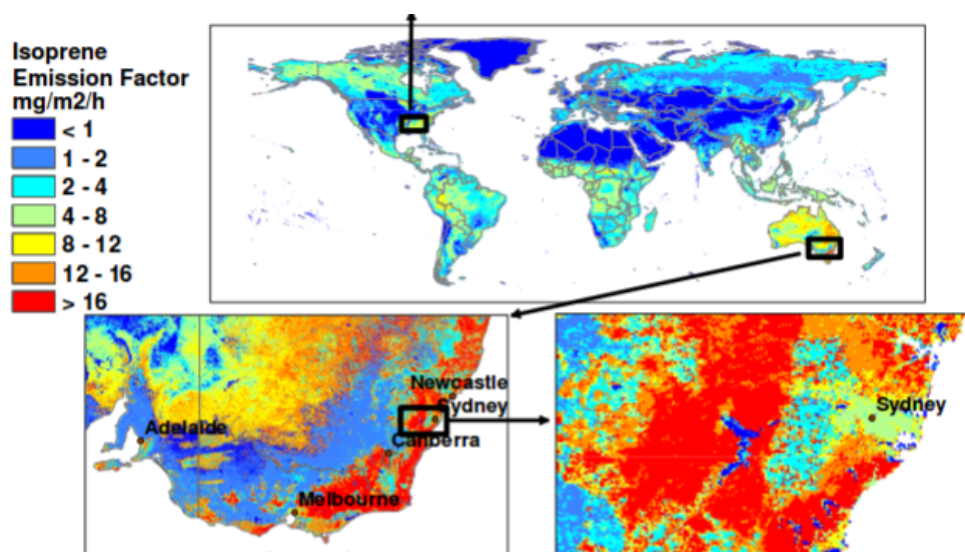


Fig. 2. Global distribution of landscape-average isoprene emission factors ($\text{mg isoprene m}^{-2} \text{h}^{-1}$). Spatial variability at the base resolution ($\sim 1 \text{ km}$) is shown by regional images of the southeastern U.S. and southeastern Australia.

FIGURE 1.9: Part of a figure from [63] showing global isoprene emission factors.

can vary heavily even within species. TODO: more on Muller2008 Australia also lacks a clear estimate of emitted monoterpenes.

[48] analyse EF sensitivity of a high resolution model of atmospheric chemistry over southeast Australia, comparing isoprene and monoterpene emissions against 4 separate campaigns. They show that the effect on total emissions is roughly linear and that no blanket EF changes are appropriate for all regions/seasons. They also mention that Australian eucalypt emissions are based on samples from young trees, which may emit more isoprene than older trees. [48] suggest that monoterpenes may be emitted in similar quantities to isoprene, with more measurements required to determine if this is so. They compare emissions estimates from MEGAN against data from several field campaigns and see overestimated isoprene emissions, as well as underestimated monoterpene emissions. Their work suggests that MEGAN estimates of isoprene emissions may be 2-6 times too high, and monoterpene emissions ~ 3 times too low over southeast Australia.

This problem is even more pronounced in Australia due to poor characterisation, or because emission factors are based on northern hemispheric data. Many plant emissions rates have not been published, such as those for any Australian acacias. Additionally soil moisture is not well quantified which has a large effect on emissions. [128] show how isoprene is poorly captured by the MEGAN model and analyse the affect of changing the soil moisture parameter, which can reduce the overall bias for Australia.

Uncertainties in isoprene emissions could explain why models of HCHO over Australia are poor at reproducing satellite measurements [169].

1.6.2 Air quality

Australian air quality is monitored independently within each state, using various metrics. These metrics are measured by varying numbers of monitoring stations in each state. In New South Wales (NSW) the metrics used to determine air quality are: particulate matter (PM), O₃, CO, NO₂, SO₂, and visibility. PM is separated into size bins: with radius < 2.5 μm and < 10 μm being PM_{2.5}, and PM₁₀ respectively. An air quality index equal to the worst of these metrics is used for NSW as shown at <http://www.environment.nsw.gov.au/aqms/aqitable.htm>. Similar methods are used in other states to get an idea of air quality. Measurement stations are generally located in population centres, and don't regularly measure precursor emissions. This is an important omission as naturally emitted precursor gases often get transported into cities where they affect air quality.

1.6.3 Measurements

TODO: Brief overview of all the measurement campaigns, pointing to Modelling and Data chapter for more details. There are relatively few measurements of isoprene in the southern hemisphere, including MUMBA(TODO CITE), other campaigns?, and very recently that girl from Macquarie University with an instrument in the daintree rainforest(TODO CITE, DESCRIBE?). For details on the MUMBA campaign see Section 2.4.1. An airflight campaign (HIPPO) measuring isoprene was also performed in 2009-2011? TODO: ask Jenny re this one.

A particulate and air quality measurement campaign took place in Sydney using PTR-MS and GC-FID, for details see Section 2.4.1.

1.7 Aims

TODO: outline of aims here (FIND THESE THEY ARE SOMEWHERE)

One of the aims in this thesis is to use the available satellite measurements to improve the estimates of isoprene emissions in Australia. Satellites which overpass daily record reflected solar (and emitted terrestrial) radiation, and give us measurements over all of Australia. Combining satellite data with model outcomes provides a platform for the understanding of natural processes which is especially useful over Australia. Due to the low availability of in-situ data over most of the Australian continent, a combination of the models with satellite can fill the gap of understanding of emissions from Australian landscapes. Improved emissions estimates will in turn improve the accuracy of CTMs, providing better predictions of atmospheric composition and its response to ongoing environmental change.

Calculation of isoprene to HCHO yields over Australia is required to create top-down estimates. This requires among other things an idea of which VOCs are present and their yields of HCHO. The technique of determining isoprene emissions from satellite detected HCHO is called satellite inversion. **Another aim to this end is to run and become familiar with GEOS-Chem in order to determine Australian emissions and yields.**

1.8 Data Access

TODO: ADD MORE HERE

OMNO2d Daily satellite NO₂ product downloaded from <https://search.earthdata.nasa.gov/search>, DOI:10.5067/Aura/OMI/DATA3007

SPEI Monthly standardised precipitation evapotranspiration index (metric to determine drought stress) downloaded from <http://hdl.handle.net/10261/153475> with DOI:10.20350/digitalCSIC/8508

OMHCHO Satellite swaths of HCHO slant columns downloaded from TODO, with DOI TODO

Bibliography

- [1] Gonzalo González Abad et al. "Smithsonian Astrophysical Observatory Ozone Mapping and Profiler Suite (SAO OMPS) formaldehyde retrieval". In: *Atmospheric Measurement Techniques* 9.7 (2016), pp. 2797–2812. ISSN: 18678548. DOI: [10.5194/amt-9-2797-2016](https://doi.org/10.5194/amt-9-2797-2016).
- [2] Dorian S. Abbot. "Seasonal and interannual variability of North American isoprene emissions as determined by formaldehyde column measurements from space". In: *Geophysical Research Letters* 30.17 (2003), pp. 1999–2002. ISSN: 0094-8276. DOI: [10.1029/2003GL017336](https://doi.org/10.1029/2003GL017336). URL: <http://doi.wiley.com/10.1029/2003GL017336>.
- [3] Dimitris Akritidis et al. "On the role of tropopause folds in summertime tropospheric ozone over the eastern Mediterranean and the Middle East". In: *Atmospheric Chemistry and Physics* 16.21 (2016), pp. 14025–14039. DOI: [10.5194/acp-16-14025-2016](https://doi.org/10.5194/acp-16-14025-2016). URL: <http://www.atmos-chem-phys.net/16/14025/2016/>.
- [4] Sebnem Aksoyoglu et al. "Secondary inorganic aerosols in Europe: sources and the significant influence of biogenic VOC emissions, especially on ammonium nitrate". In: *Atmospheric Chemistry and Physics* 17.12 (2017), pp. 7757–7773. ISSN: 1680-7324. DOI: [10.5194/acp-17-7757-2017](https://doi.org/10.5194/acp-17-7757-2017). URL: <https://www.atmos-chem-phys.net/17/7757/2017/>.
- [5] S. P. Alexander et al. "High resolution VHF radar measurements of tropopause structure and variability at Davis, Antarctica (69 S, 78 E)". In: *Atmospheric Chemistry and Physics* 13.6 (2013), pp. 3121–3132. ISSN: 16807324. DOI: [10.5194/acp-13-3121-2013](https://doi.org/10.5194/acp-13-3121-2013). URL: <http://www.atmos-chem-phys.net/13/3121/2013/>.
- [6] M O Andreae. "Emission of trace gases and aerosols from biomass burning". In: *Biogeochemistry* 15.4 (2001), pp. 955–966. URL: <http://onlinelibrary.wiley.com/doi/10.1029/2000GB001382/epdf>.
- [7] A Arneth et al. "Why are estimates of global terrestrial isoprene emissions so similar (and why is this not so for monoterpenes)?" In: *Atmos. Chem. Phys* 8.x (2008), pp. 4605–4620. ISSN: 1680-7375. DOI: [10.5194/acpd-8-7017-2008](https://doi.org/10.5194/acpd-8-7017-2008).
- [8] Almut Arneth et al. "CO₂ inhibition of global terrestrial isoprene emissions: Potential implications for atmospheric chemistry". In: *Geophysical Research Letters* 34.18 (2007), p. L18813. DOI: [10.1029/2007GL030615](https://doi.org/10.1029/2007GL030615). URL: <http://doi.wiley.com/10.1029/2007GL030615>.
- [9] M R Ashmore, Lisa Emberson, and Murray Frank. *Air pollution impacts on crops and forests : a global assessment*. Ed. by Lisa Emberson, Mike Ashmore, and Frank Murray. Imperial College Press London ; River Edge, NJ, 2003, xiii, 372 p. : ISBN: 186094292.

- [10] Roger Atkinson. "Atmospheric chemistry of VOCs and NO(x)". In: *Atmospheric Environment* 34.12-14 (2000), pp. 2063–2101. ISSN: 13522310. DOI: [10.1016/S1352-2310\(99\)00460-4](https://doi.org/10.1016/S1352-2310(99)00460-4).
- [11] Roger Atkinson and Janet Arey. "Gas-phase tropospheric chemistry of biogenic volatile organic compounds: A review". In: *Atmospheric Environment* 37.SUPPL. 2 (2003). ISSN: 13522310. DOI: [10.1016/S1352-2310\(03\)00391-1](https://doi.org/10.1016/S1352-2310(03)00391-1).
- [12] Shiri Avnery et al. "Global crop yield reductions due to surface ozone exposure: 2. Year 2030 potential crop production losses and economic damage under two scenarios of O₃ pollution". In: *Atmospheric Environment* 71.13 (2013), pp. 408–409. ISSN: 13522310. DOI: [10.1016/j.atmosenv.2012.12.045](https://doi.org/10.1016/j.atmosenv.2012.12.045). URL: <http://dx.doi.org/10.1016/j.atmosenv.2011.01.002>.
- [13] James D Ayers and William R Simpson. "Measurements of N₂O₅ near Fairbanks, Alaska". In: *Journal of Geophysical Research: Atmospheres* 111.D14 (2006), n/a–n/a. ISSN: 2156-2202. DOI: [10.1029/2006JD007070](https://doi.org/10.1029/2006JD007070). URL: <http://dx.doi.org/10.1029/2006JD007070>.
- [14] J. L. Baray et al. "Planetary-scale tropopause folds in the southern subtropics". In: *Geophysical Research Letters* 27.3 (2000), pp. 353–356. ISSN: 00948276. DOI: [10.1029/1999GL010788](https://doi.org/10.1029/1999GL010788).
- [15] Jean-Luc Baray et al. "One year ozonesonde measurements at Kerguelen Island (49.2S, 70.1E): Influence of stratosphere-to-troposphere exchange and long-range transport of biomass burning plumes". In: *Journal of Geophysical Research* 117.D6 (2012). ISSN: 2156-2202. DOI: [10.1029/2011JD016717](https://doi.org/10.1029/2011JD016717). URL: <http://dx.doi.org/10.1029/2011JD016717>.
- [16] Michael P. Barkley et al. "Top-down isoprene emissions over tropical South America inferred from SCIAMACHY and OMI formaldehyde columns". In: *Journal of Geophysical Research Atmospheres* 118.12 (2013), pp. 6849–6868. ISSN: 21698996. DOI: [10.1002/jgrd.50552](https://doi.org/10.1002/jgrd.50552). URL: <http://dx.doi.org/10.1002/jgrd.50552>.
- [17] M Bauwens et al. "Satellite-based isoprene emission estimates (2007–2012) from the GlobEmission project". In: *Proceedings of the ACCENT-Plus Symposium, Atmospheric Composition Change-Policy Support and Science, Urbino*. 2013, pp. 17–20.
- [18] Maite Bauwens et al. "Nine years of global hydrocarbon emissions based on source inversion of OMI formaldehyde observations". In: *Atmospheric Chemistry and Physics Discussions* March (2016), pp. 1–45. ISSN: 1680-7375. DOI: [10.5194/acp-2016-221](https://doi.org/10.5194/acp-2016-221). URL: <http://www.atmos-chem-phys-discuss.net/acp-2016-221/>.
- [19] M. Beekmann et al. "Regional and global tropopause fold occurrence and related ozone flux across the tropopause". In: *Journal of Atmospheric Chemistry* 28.1-3 (1997), pp. 29–44. ISSN: 01677764. DOI: [10.1023/A:1005897314623](https://doi.org/10.1023/A:1005897314623).

- [20] N Bei, G Li, and L T Molina. "Uncertainties in SOA simulations due to meteorological uncertainties in Mexico City during MILAGRO-2006 field campaign". In: *Atmospheric Chemistry and Physics* 12.23 (2012), pp. 11295–11308. DOI: [10.5194/acp-12-11295-2012](https://doi.org/10.5194/acp-12-11295-2012). URL: <http://www.atmos-chem-phys.net/12/11295/2012/>.
- [21] S. Bethan, G. Vaughan, and S. J. Reid. "A comparison of ozone and thermal tropopause heights and the impact of tropopause definition on quantifying the ozone content of the troposphere". In: *Quarterly Journal of the Royal Meteorological Society* 122.532 (1996), pp. 929–944. ISSN: 00359009. DOI: [10.1002/qj.49712253207](https://doi.org/10.1002/qj.49712253207). URL: <http://doi.wiley.com/10.1002/qj.49712253207>.
- [22] Isabelle Bey et al. "Global Modeling of Tropospheric Chemistry with Assimilated Meteorology: Model Description and Evaluation". In: *Journal of Geophysical Research* 106 (2001), pp. 73–95. ISSN: 0148-0227. DOI: [10.1029/2001JD000807](https://doi.org/10.1029/2001JD000807).
- [23] E. J. Brinksmma et al. "Five years of observations of ozone profiles over Lauder, New Zealand". In: *Journal of Geophysical Research* 107.D14 (2002), pp. 1–11. ISSN: 0148-0227. DOI: [10.1029/2001JD000737](https://doi.org/10.1029/2001JD000737). URL: <http://doi.wiley.com/10.1029/2001JD000737>.
- [24] S. S. Brown et al. "Nocturnal isoprene oxidation over the Northeast United States in summer and its impact on reactive nitrogen partitioning and secondary organic aerosol". In: *Atmospheric Chemistry and Physics* 9.9 (2009), pp. 3027–3042. ISSN: 16807316. DOI: [10.5194/acp-9-3027-2009](https://doi.org/10.5194/acp-9-3027-2009).
- [25] K. Chance et al. "Satellite observations of formaldehyde over North America from GOME". In: *Geophysical Research Letters* 27.21 (2000), pp. 3461–3464. ISSN: 00948276. DOI: [10.1029/2000GL011857](https://doi.org/10.1029/2000GL011857). URL: <http://dx.doi.org/10.1029/2000gl011857>.
- [26] D. Chen et al. "Regional CO pollution in China simulated by the high-resolution nested-grid GEOS-Chem model". In: *Atmospheric Chemistry and Physics Discussions* 9.2 (2009), pp. 5853–5887. ISSN: 1680-7324. DOI: [10.5194/acpd-9-5853-2009](https://doi.org/10.5194/acpd-9-5853-2009). URL: <http://dx.doi.org/10.5194/acp-9-3825-2009>.
- [27] F. Chevallier et al. "The formaldehyde budget as seen by a global-scale multi-constraint and multi-species inversion system". In: *Atmospheric Chemistry and Physics* 12.15 (2012), pp. 6699–6721. ISSN: 16807316. DOI: [10.5194/acp-12-6699-2012](https://doi.org/10.5194/acp-12-6699-2012). URL: <http://www.atmos-chem-phys.net/12/6699/2012/acp-12-6699-2012.pdf>.
- [28] Kenneth E Christian, William H Brune, and Jingqiu Mao. "Global sensitivity analysis of the GEOS-Chem chemical transport model: ozone and hydrogen oxides during ARCTAS (2008)". In: *Atmos. Chem. Phys* 17 (2017), pp. 3769–3784. DOI: [10.5194/acp-17-3769-2017](https://doi.org/10.5194/acp-17-3769-2017). URL: www.atmos-chem-phys.net/17/3769/2017/.
- [29] O. Cooper et al. "On the life cycle of a stratospheric intrusion and its dispersion into polluted warm conveyor belts". In: *Journal of Geophysical Research* 109.23 (2004), pp. 1–18. ISSN: 01480227. DOI: [10.1029/2003JD004006](https://doi.org/10.1029/2003JD004006).

- [30] John D Crounse et al. "Peroxy radical isomerization in the oxidation of isoprene". In: *Physical Chemistry Chemical Physics* 13.30 (2011), pp. 13607–13613. ISSN: 1463-9076. DOI: [doi:10.1039/c1cp21330j](https://doi.org/10.1039/c1cp21330j). URL: <http://dx.doi.org/10.1039/C1CP21330J>.
- [31] John D Crounse et al. "Atmospheric Fate of Methacrolein. 1. Peroxy Radical Isomerization Following Addition of OH and O₂". In: *Physical Chemistry m* (2012).
- [32] John D. Crounse et al. "Autoxidation of organic compounds in the atmosphere". In: *Journal of Physical Chemistry Letters* 4.20 (2013), pp. 3513–3520. ISSN: 19487185. DOI: [10.1021/jz4019207](https://doi.org/10.1021/jz4019207). URL: <http://pubs.acs.org/doi/abs/10.1021/jz4019207>.
- [33] PAUL J CRUTZEN, MARK G LAWRENCE, and ULRICH PÖSCHL. "On the background photochemistry of tropospheric ozone". In: *Tellus A* 51.1 (1999), pp. 123–146. ISSN: 1600-0870. DOI: [10.1034/j.1600-0870.1999.t01-1-00010.x](https://doi.org/10.1034/j.1600-0870.1999.t01-1-00010.x). URL: <http://dx.doi.org/10.1034/j.1600-0870.1999.t01-1-00010.x>.
- [34] G. Curci et al. "Estimating European volatile organic compound emissions using satellite observations of formaldehyde from the Ozone Monitoring Instrument". In: *Atmospheric Chemistry and Physics* 10.23 (2010), pp. 11501–11517. ISSN: 16807316. DOI: [10.5194/acp-10-11501-2010](https://doi.org/10.5194/acp-10-11501-2010).
- [35] Edwin F. Danielsen. *Stratospheric-Tropospheric Exchange Based on Radioactivity, Ozone and Potential Vorticity*. 1968. DOI: [10.1175/1520-0469\(1968\)025<0502:STEBOR>2.0.CO;2](https://doi.org/10.1175/1520-0469(1968)025<0502:STEBOR>2.0.CO;2).
- [36] Siddarth Shankar Das et al. "Influence of tropical cyclones on tropospheric ozone: possible implications". In: *Atmospheric Chemistry and Physics* 16 (2016), pp. 4837–4847. DOI: [10.5194/acp-16-4837-2016](https://doi.org/10.5194/acp-16-4837-2016). URL: www.atmos-chem-phys.net/16/4837/2016/.
- [37] J. J. Davenport et al. "A measurement strategy for non-dispersive ultra-violet detection of formaldehyde in indoor air: spectral analysis and interferent gases". In: *Measurement Science and Technology* 015802. December 2015 (2015), p. 15802. ISSN: 0957-0233. DOI: [10.1088/0957-0233/27/1/015802](https://doi.org/10.1088/0957-0233/27/1/015802). URL: <http://dx.doi.org/10.1088/0957-0233/27/1/015802>.
- [38] I De Smedt et al. "Twelve years of global observations of formaldehyde in the troposphere using GOME and SCIAMACHY sensors". In: *Atmos. Chem. Phys.* 8.16 (2008), pp. 4947–4963. ISSN: 1680-7324. DOI: [10.5194/acp-8-4947-2008](https://doi.org/10.5194/acp-8-4947-2008). URL: <http://www.atmos-chem-phys.net/8/4947/2008/>.
- [39] I. De Smedt et al. "Improved retrieval of global tropospheric formaldehyde columns from GOME-2/MetOp-A addressing noise reduction and instrumental degradation issues". In: *Atmospheric Measurement Techniques* 5.11 (2012), pp. 2933–2949. ISSN: 18671381. DOI: [10.5194/amt-5-2933-2012](https://doi.org/10.5194/amt-5-2933-2012).

- [40] I. De Smedt et al. "Diurnal, seasonal and long-term variations of global formaldehyde columns inferred from combined OMI and GOME-2 observations". In: *Atmospheric Chemistry and Physics* 15.21 (2015), pp. 12519–12545. ISSN: 16807324. DOI: [10.5194/acp-15-12519-2015](https://doi.org/10.5194/acp-15-12519-2015). URL: <http://www.atmos-chem-phys-discuss.net/15/12241/2015/%5Cnhttp://www.atmos-chem-phys-discuss.net/15/12241/2015/acpd-15-12241-2015.pdf>.
- [41] D P Dee et al. "The ERA-Interim reanalysis: configuration and performance of the data assimilation system". In: *Quarterly Journal of the Royal Meteorological Society* 137.656 (2011), pp. 553–597. ISSN: 1477-870X. DOI: [10.1002/qj.828](https://doi.org/10.1002/qj.828). URL: <http://dx.doi.org/10.1002/qj.828>.
- [42] G. Dufour et al. "SCIAMACHY formaldehyde observations: constraint for isoprene emissions over Europe?" In: *Atmospheric Chemistry and Physics* 8.6 (2008), pp. 19273–19312. ISSN: 1680-7324. DOI: [10.5194/acpd-8-19273-2008](https://doi.org/10.5194/acpd-8-19273-2008).
- [43] Erin Dunne et al. "Comparison of VOC measurements made by PTR-MS, Adsorbent Tube/GC-FID-MS and DNPH-derivatization/HPLC during the Sydney Particle Study, 2012: a contribution to the assessment of uncertainty in current atmospheric VOC measurements". In: *Atmospheric Measurement Techniques Discussions* (2017), pp. 1–24. ISSN: 1867-8610. DOI: [10.5194/amt-2016-349](https://doi.org/10.5194/amt-2016-349). URL: <https://www.atmos-meas-tech-discuss.net/amt-2016-349/>.
- [44] Sebastian D. Eastham, Debra K. Weisenstein, and Steven R H Barrett. "Development and evaluation of the unified tropospheric-stratospheric chemistry extension (UCX) for the global chemistry-transport model GEOS-Chem". In: *Atmospheric Environment* 89 (2014), pp. 52–63. ISSN: 13522310. DOI: [10.1016/j.atmosenv.2014.02.001](https://doi.org/10.1016/j.atmosenv.2014.02.001). URL: <http://dx.doi.org/10.1016/j.atmosenv.2014.02.001>.
- [45] D. P. Edwards. "Tropospheric ozone over the tropical Atlantic: A satellite perspective". In: *Journal of Geophysical Research* 108.D8 (2003), p. 4237. ISSN: 0148-0227. DOI: [10.1029/2002JD002927](https://doi.org/10.1029/2002JD002927). URL: <http://doi.wiley.com/10.1029/2002JD002927>.
- [46] D. P. Edwards et al. "Satellite-observed pollution from Southern Hemisphere biomass burning". In: *Journal of Geophysical Research* 111.14 (2006), pp. 1–17. ISSN: 01480227. DOI: [10.1029/2005JD006655](https://doi.org/10.1029/2005JD006655).
- [47] H Elbern, J Hendricks, and A Ebel. "A Climatology of Tropopause Folds by Global Analyses". In: *Theoretical and Applied Climatology* 59.3 (1998), pp. 181–200. ISSN: 1434-4483. DOI: [10.1007/s007040050023](https://doi.org/10.1007/s007040050023). URL: <http://dx.doi.org/10.1007/s007040050023>.
- [48] Kathryn M. Emmerson et al. "Current estimates of biogenic emissions from eucalypts uncertain for southeast Australia". In: *Atmospheric Chemistry and Physics* 16.11 (2016), pp. 6997–7011. ISSN: 1680-7324. DOI: [10.5194/acp-16-6997-2016](https://doi.org/10.5194/acp-16-6997-2016). URL: <http://www.atmos-chem-phys.net/16/6997/2016/>.
- [49] H J Eskes and K F Boersma. "Averaging kernels for DOAS total-column satellite retrievals". In: *Atmospheric Chemistry and Physics* 3.1 (2003), pp. 1285–1291. ISSN: 1680-7324. DOI: [10.5194/acp-3-1285-2003](https://doi.org/10.5194/acp-3-1285-2003). URL: <http://dx.doi.org/10.5194/acpd-3-895-2003>.

- [50] EUMETSAT. GOME2. 2015. URL: <http://www.eumetsat.int/website/home/Satellites/CurrentSatellites/Metop/MetopDesign/GOME2/index.html>.
- [51] Jiwen Fan and Renyi Zhang. "Atmospheric oxidation mechanism of isoprene". In: *Environmental Chemistry* 1.3 (2004), pp. 140–149. ISSN: 14482517. DOI: [10.1071/EN04045](https://doi.org/10.1071/EN04045). URL: <http://dx.doi.org/10.1071/en04045>.
- [52] P. Forster et al. *Changes in Atmospheric Constituents and in Radiative Forcing*. In: *Climate Change 2007: The Physical Science Basis. Contribution of Working Group I to the Fourth Assessment Report of the Intergovernmental Panel on Climate Change* [Solomon, S., D. Qin, M. Man. 2007. URL: https://www.ipcc.ch/publications_and_data/ar4/wg1/en/ch2.html (visited on 01/14/2016).
- [53] B. Franco et al. "Retrievals of formaldehyde from ground-based FTIR and MAX-DOAS observations at the Jungfraujoch station and comparisons with GEOS-Chem and IMAGES model simulations". In: *Atmospheric Measurement Techniques* 8.4 (2015), pp. 1733–1756. ISSN: 18678548. DOI: [10.5194/amt-8-1733-2015](https://doi.org/10.5194/amt-8-1733-2015).
- [54] W. Frey et al. "The impact of overshooting deep convection on local transport and mixing in the tropical upper troposphere/lower stratosphere (UTLS)". In: *Atmospheric Chemistry and Physics* 15.11 (2015), pp. 6467–6486. ISSN: 1680-7324. DOI: [10.5194/acp-15-6467-2015](https://doi.org/10.5194/acp-15-6467-2015). URL: <http://www.atmos-chem-phys.net/15/6467/2015/>.
- [55] Tzung-may Fu et al. "Space-based formaldehyde measurements as constraints on volatile organic compound emissions in east and south Asia and implications for ozone". In: 112 (2007), pp. 1–15. DOI: [10.1029/2006JD007853](https://doi.org/10.1029/2006JD007853).
- [56] J. D. Fuentes et al. "Biogenic Hydrocarbons in the Atmospheric Boundary Layer: A Review". In: *Bulletin of the American Meteorological Society* 81.7 (2000), pp. 1537–1575. ISSN: 00030007. DOI: [10.1175/1520-0477\(2000\)081<1537:BHITAB>2.3.CO;2](https://doi.org/10.1175/1520-0477(2000)081<1537:BHITAB>2.3.CO;2). arXiv: [arXiv:1011.1669v3](https://arxiv.org/abs/1011.1669v3). URL: [http://journals.ametsoc.org/doi/abs/10.1175/1520-0477\(2000\)081%3C1537%3ABHITAB%3E2.3.CO%3B2](http://journals.ametsoc.org/doi/abs/10.1175/1520-0477(2000)081%3C1537%3ABHITAB%3E2.3.CO%3B2).
- [57] E. Galani. "Observations of stratosphere-to-troposphere transport events over the eastern Mediterranean using a ground-based lidar system". In: *Journal of Geophysical Research* 108.D12 (2003), pp. 1–10. ISSN: 0148-0227. DOI: [10.1029/2002JD002596](https://doi.org/10.1029/2002JD002596). URL: <http://www.agu.org/pubs/crossref/2003/2002JD002596.shtml>.
- [58] Louis Giglio, Ivan Csiszar, and Christopher O. Justice. "Global distribution and seasonality of active fires as observed with the Terra and Aqua Moderate Resolution Imaging Spectroradiometer (MODIS) sensors". In: *Journal of Geophysical Research: Biogeosciences* 111.2 (2006), pp. 1–12. ISSN: 01480227. DOI: [10.1029/2005JG000142](https://doi.org/10.1029/2005JG000142).
- [59] Louis Giglio, James T. Randerson, and Guido R. Van Der Werf. "Analysis of daily, monthly, and annual burned area using the fourth-generation global fire emissions database (GFED4)". In: *Journal of Geophysical Research* 118.1 (2013), pp. 317–328. ISSN: 21698961. DOI: [10.1002/jgrg.20042](https://doi.org/10.1002/jgrg.20042).

- [60] Marianne Glasius and Allen H. Goldstein. "Recent Discoveries and Future Challenges in Atmospheric Organic Chemistry". In: *Environmental Science and Technology* 50.6 (2016), pp. 2754–2764. ISSN: 15205851. DOI: [10.1021/acs.est.5b05105](https://doi.org/10.1021/acs.est.5b05105).
- [61] Annemieke Gloudemans et al. "Evidence for long-range transport of carbon monoxide in the Southern Hemisphere from SCIAMACHY observations". In: *European Space Agency, (Special Publication)* 33.SP-636 (2007), pp. 1–5. ISSN: 03796566. DOI: [10.1029/2006GL026804](https://doi.org/10.1029/2006GL026804).
- [62] G. Gonzalez Abad et al. "Updated Smithsonian Astrophysical Observatory Ozone Monitoring Instrument (SAO OMI) formaldehyde retrieval". In: *Atmospheric Measurement Techniques* 8.1 (2015), pp. 19–32. ISSN: 18678548. DOI: [10.5194/amt-8-19-2015](https://doi.org/10.5194/amt-8-19-2015).
- [63] A Guenther et al. "Estimates of global terrestrial isoprene emissions using MEGAN (Model of Emissions of Gases and Aerosols from Nature)". In: *Atmospheric Chemistry and Physics* 6.11 (2006), pp. 3181–3210. DOI: [10.5194/acp-6-3181-2006](https://doi.org/10.5194/acp-6-3181-2006). URL: <http://dx.doi.org/10.5194/acp-6-3181-2006>.
- [64] A. B. Guenther et al. "The model of emissions of gases and aerosols from nature version 2.1 (MEGAN2.1): An extended and updated framework for modeling biogenic emissions". In: *Geoscientific Model Development* 5.6 (2012), pp. 1471–1492. ISSN: 1991959X. DOI: [10.5194/gmd-5-1471-2012](https://doi.org/10.5194/gmd-5-1471-2012).
- [65] Alex Guenther. MEGAN. 2016. URL: <http://lar.wsu.edu/megan/>.
- [66] Alex Guenther et al. "A global model of natural volatile organic compound emissions". In: *Journal of Geophysical Research* 100.D5 (1995), pp. 8873–8892. ISSN: 0148-0227. DOI: [10.1029/94JD02950](https://doi.org/10.1029/94JD02950). URL: <http://onlinelibrary.wiley.com/doi/10.1029/94JD02950/full><http://doi.wiley.com/10.1029/94JD02950><http://onlinelibrary.wiley.com/doi/10.1029/94JD02950/full>.
- [67] Alex Guenther et al. "Natural emissions of non-methane volatile organic compounds, carbon monoxide, and oxides of nitrogen from North America". In: *Atmospheric Environment* 34.12-14 (2000), pp. 2205–2230. ISSN: 13522310. DOI: [10.1016/S1352-2310\(99\)00465-3](https://doi.org/10.1016/S1352-2310(99)00465-3).
- [68] C. Hak et al. "Intercomparison of four different in-situ techniques for ambient formaldehyde measurements in urban air". In: *Atmospheric Chemistry and Physics Discussions* 5.3 (2005), pp. 2897–2945. ISSN: 1680-7316. DOI: [10.5194/acpd-5-2897-2005](https://doi.org/10.5194/acpd-5-2897-2005).
- [69] Michaela I Hegglin and Theodore G Shepherd. "Large climate-induced changes in ultraviolet index and stratosphere-to-troposphere ozone flux". In: *Nature Geoscience* 2.10 (2009), pp. 687–691. DOI: [10.1038/ngeo604](https://doi.org/10.1038/ngeo604). URL: <http://dx.doi.org/10.1038/ngeo604>.
- [70] C N Hewitt et al. "Ground-level ozone influenced by circadian control of isoprene emissions". In: *Nature Geoscience* 4.10 (2011), pp. 671–674. DOI: [10.1038/ngeo1271](https://doi.org/10.1038/ngeo1271). URL: <http://dx.doi.org/10.1038/ngeo1271>.
- [71] Gerard Hoek et al. "Long-term air pollution exposure and cardio- respiratory mortality: a review". In: *Environmental Health* 12.1 (2013), p. 43. DOI: [10.1186/1476-069x-12-43](https://doi.org/10.1186/1476-069x-12-43). URL: <http://dx.doi.org/10.1186/1476-069x-12-43>.

- [72] Larry W. Horowitz et al. "Export of reactive nitrogen from North America during summertime: Sensitivity to hydrocarbon chemistry". In: *Journal of Geophysical Research* 103.D11 (1998), pp. 13451–13476. ISSN: 0148-0227. DOI: [10.1029/97JD03142](https://doi.org/10.1029/97JD03142). URL: <http://doi.wiley.com/10.1029/97JD03142><http://www.agu.org/pubs/crossref/1998/97JD03142.shtml>.
- [73] Nan-Hung Hsieh and Chung-Min Liao. "Fluctuations in air pollution give risk warning signals of asthma hospitalization". In: *Atmospheric Environment* 75 (2013), pp. 206–216. DOI: [10.1016/j.atmosenv.2013.04.043](https://doi.org/10.1016/j.atmosenv.2013.04.043). URL: <http://dx.doi.org/10.1016/j.atmosenv.2013.04.043>.
- [74] Lu Hu et al. "Global budget of tropospheric ozone: evaluating recent model advances with satellite (OMI), aircraft (IAGOS), and ozonesonde observations". In: *Atmospheric Environment* (2017), pp. 1–36. DOI: [10.1016/j.atmosenv.2017.08.036](https://doi.org/10.1016/j.atmosenv.2017.08.036).
- [75] Guanyu Huang et al. "Validation of 10-year SAO OMI Ozone Profile (PRO-FOZ) Product Using Aura MLS Measurements". In: *Atmospheric Measurement Techniques Discussions* (2017), pp. 1–25. ISSN: 1867-8610. DOI: [10.5194/amt-2017-92](https://doi.org/10.5194/amt-2017-92). URL: <https://www.atmos-meas-tech-discuss.net/amt-2017-92/>.
- [76] OMI Instrument. "OMI Algorithm Theoretical Basis Document Volume I". In: I.August (2002), pp. 1–50.
- [77] Intergovernmental Panel on Climate Change (IPCC): *Climate Change: The Scientific Basis*. Tech. rep. Cambridge University Press, 2001. URL: <http://www.ipcc.ch/ipccreports/tar/>.
- [78] Daniel J Jacob. *Introduction to Atmospheric Chemistry*. Ed. by Daniel J Jacob. Princeton University Press, 1999. URL: <http://acmg.seas.harvard.edu/people/faculty/djj/book/index.html>.
- [79] M C Jacobson and H Hansson. "Organic atmospheric aerosols: Review and state of the science". In: *Reviews of Geophysics* 38.38 (2000), pp. 267–294. ISSN: 87551209. DOI: [10.1029/1998RG000045](https://doi.org/10.1029/1998RG000045). URL: <http://dx.doi.org/10.1029/1998RG000045>.
- [80] Daniel a. Jaffe and Nicole L. Wigder. "Ozone production from wildfires: A critical review". In: *Atmospheric Environment* 51 (2012), pp. 1–10. ISSN: 13522310. DOI: [10.1016/j.atmosenv.2011.11.063](https://doi.org/10.1016/j.atmosenv.2011.11.063). URL: <http://dx.doi.org/10.1016/j.atmosenv.2011.11.063>.
- [81] P Jöckel et al. "The atmospheric chemistry general circulation model ECHAM5/MESy1: consistent simulation of ozone from the surface to the mesosphere". In: *Atmospheric Chemistry and Physics* 6.12 (2006), pp. 5067–5104. DOI: [10.5194/acp-6-5067-2006](https://doi.org/10.5194/acp-6-5067-2006). URL: <http://www.atmos-chem-phys.net/6/5067/2006/>.
- [82] Patrick Jöckel, Rolf Sander, and Jos Lelieveld. "Technical Note: The Modular Earth Submodel System (MESSy) – a new approach towards Earth System Modeling". In: *Atmospheric Chemistry and Physics Discussions* 4.6 (2004), pp. 7139–7166. ISSN: 1680-7324. DOI: [10.5194/acpd-4-7139-2004](https://doi.org/10.5194/acpd-4-7139-2004).
- [83] Peeters Jozef et al. "Hydroxyl Radical Recycling in Isoprene Oxidation Driven by Hydrogen Bonding and Hydrogen Tunneling: The Upgraded LIM1 Mechanism". In: *Journal of Physical Chemistry* (2014).

- [84] M Kanakidou et al. "Physics Organic aerosol and global climate modelling : a review". In: *Atmospheric Chemistry and Physics* 5 (2005), pp. 1053–1123.
- [85] Shawn C. Kefauver, Iolanda Filella, and Josep Peñuelas. "Remote sensing of atmospheric biogenic volatile organic compounds (BVOCs) via satellite-based formaldehyde vertical column assessments". en. In: *International Journal of Remote Sensing* (2014). URL: <http://www.tandfonline.com/doi/abs/10.1080/01431161.2014.968690#.VkqEubNM61M>.
- [86] D Krewski et al. "Extended follow-up and spatial analysis of the American Cancer Society study linking particulate air pollution and mortality". In: *Res Rep Health Eff Inst* 140 (2009), pp. 5–36. ISSN: 1041-5505 (Print) 1041-5505 (Linking). URL: <http://www.ncbi.nlm.nih.gov/pubmed/19627030>.
- [87] Jesse H. Kroll and John H. Seinfeld. "Chemistry of secondary organic aerosol: Formation and evolution of low-volatility organics in the atmosphere". In: *Atmospheric Environment* 42.16 (2008), pp. 3593–3624. ISSN: 13522310. DOI: 10.1016/j.atmosenv.2008.01.003. URL: <http://www.sciencedirect.com.ezproxy.uow.edu.au/science/article/pii/S1352231008000253>.
- [88] Shi Kuang et al. "Summertime tropospheric ozone enhancement associated with a cold front passage due to stratosphere-to-troposphere transport and biomass burning: Simultaneous ground-based lidar and airborne measurements". In: *Journal of Geophysical Research: Atmospheres* 122.2 (2017), pp. 1293–1311. ISSN: 21698996. DOI: 10.1002/2016JD026078. URL: <http://doi.wiley.com/10.1002/2016JD026078>.
- [89] T Kurosu and K Chance. *OMIReadme*. 2014. URL: https://www.cfa.harvard.edu/atmosphere/Instruments/OMI/PGEReleases/READMEs/OMHCHO_README_v3.0.pdf.
- [90] Hyeong-Ahn Kwon et al. "Sensitivity of formaldehyde (HCHO) column measurements from a geostationary satellite to temporal variation of the air mass factor in East Asia". In: *Atmospheric Chemistry and Physics* 17.7 (2017), pp. 4673–4686. ISSN: 1680-7324. DOI: 10.5194/acp-17-4673-2017. URL: <http://www.atmos-chem-phys.net/17/4673/2017/>.
- [91] L N Lamsal et al. "Evaluation of OMI operational standard NO₂ column retrievals using in situ and surface-based NO₂ observations". In: *Atmos. Chem. Phys* 14 (2014), pp. 11587–11609. DOI: 10.5194/acp-14-11587-2014. URL: www.atmos-chem-phys.net/14/11587/2014/.
- [92] A. O. Langford et al. "Stratospheric influence on surface ozone in the Los Angeles area during late spring and early summer of 2010". In: *Journal of Geophysical Research* 117.3 (2012), pp. 1–17. ISSN: 01480227. DOI: 10.1029/2011JD016766.
- [93] J Lathière et al. "Impact of climate variability and land use changes on global biogenic volatile organic compound emissions". In: *Atmospheric Chemistry and Physics* 6.2003 (2006), pp. 2129–2146. ISSN: 16807324. DOI: 10.5194/acp-6-2129-2006. URL: www.atmos-chem-phys.net/6/2129/2006/.
- [94] Anita Lee et al. "Gas-phase products and secondary aerosol yields from the photooxidation of 16 different terpenes". In: *Journal of Geophysical Research Atmospheres* 111.17 (2006), pp. 1–18. ISSN: 01480227. DOI: 10.1029/2006JD007050.

- [95] Hanlim Lee et al. "Investigations of the Diurnal Variation of Vertical HCHO Profiles Based on MAX-DOAS Measurements in Beijing: Comparisons with OMI Vertical Column Data". In: *Atmosphere* (2015). URL: [10.3390/atmos6111816](https://doi.org/10.3390/atmos6111816).
- [96] Allen S. Lefohn et al. "The importance of stratospheric-tropospheric transport in affecting surface ozone concentrations in the western and northern tier of the United States". In: *Atmospheric Environment* 45.28 (2011), pp. 4845–4857. ISSN: 13522310. DOI: [10.1016/j.atmosenv.2011.06.014](https://doi.org/10.1016/j.atmosenv.2011.06.014). URL: <http://dx.doi.org/10.1016/j.atmosenv.2011.06.014>.
- [97] J. Lelieveld et al. "Severe ozone air pollution in the Persian Gulf region". In: *Atmospheric Chemistry and Physics* 9 (2009), pp. 1393–1406. ISSN: 1680-7324. DOI: [10.5194/acp-9-1393-2009](https://doi.org/10.5194/acp-9-1393-2009).
- [98] J Lelieveld et al. "The contribution of outdoor air pollution sources to premature mortality on a global scale". In: *Nature* 525.7569 (2015), pp. 367–371. DOI: [10.1038/nature15371](https://doi.org/10.1038/nature15371). URL: <http://dx.doi.org/10.1038/nature15371>.
- [99] Jos Lelieveld and Frank J. Dentener. "What controls tropospheric ozone?" In: *Journal of Geophysical Research* 105.D3 (2000), pp. 3531–3551. ISSN: 01480227. DOI: [10.1029/1999JD901011](https://doi.org/10.1029/1999JD901011). URL: <http://doi.wiley.com/10.1029/1999JD901011>.
- [100] C Leue et al. "Quantitative analysis of NO_x emissions from Global Ozone Monitoring Experiment satellite image sequences". In: *J. Geophys. Res.* 106.D6 (2001), p. 5493. DOI: [10.1029/2000jd900572](https://doi.org/10.1029/2000jd900572). URL: <http://dx.doi.org/10.1029/2000jd900572>.
- [101] Hiram Levy. "Photochemistry of the lower troposphere". In: *Planetary and Space Science* 20.6 (1972), pp. 919–935. ISSN: 00320633. DOI: [10.1016/0032-0633\(72\)90177-8](https://doi.org/10.1016/0032-0633(72)90177-8).
- [102] Meiyun Lin et al. "Springtime high surface ozone events over the western United States: Quantifying the role of stratospheric intrusions". In: *Journal of Geophysical Research* 117.19 (2012), pp. 1–20. ISSN: 01480227. DOI: [10.1029/2012JD018151](https://doi.org/10.1029/2012JD018151).
- [103] Meiyun Lin et al. "Climate variability modulates western US ozone air quality in spring via deep stratospheric intrusions." In: *Nature communications* 6.May (2015), p. 7105. ISSN: 2041-1723. DOI: [10.1038/ncomms8105](https://doi.org/10.1038/ncomms8105). URL: <http://www.nature.com/ncomms/2015/150512/ncomms8105/full/ncomms8105.html>.
- [104] Ying-Hsuan Lin et al. "Epoxide as a precursor to secondary organic aerosol formation from isoprene photooxidation in the presence of nitrogen oxides". In: (2013). DOI: [10.1073/pnas.1221150110](https://doi.org/10.1073/pnas.1221150110). URL: <http://www.pnas.org/content/110/17/6718.full.pdf>.
- [105] Junhua Liu et al. "Origins of tropospheric ozone interannual variation over Réunion: A model investigation". In: *Journal of Geophysical Research* (2015), pp. 1–19. DOI: [10.1002/2015JD023981](https://doi.org/10.1002/2015JD023981). URL: <http://onlinelibrary.wiley.com/doi/10.1002/2015JD023981/abstract>.
- [106] Junhua Liu et al. "Causes of interannual variability of tropospheric ozone over the Southern Ocean". In: *Atmospheric Chemistry and Physics Discussions* October (2016), pp. 1–46. ISSN: 1680-7316. DOI: [10.5194/ACP-2016-692](https://doi.org/10.5194/ACP-2016-692).

- [107] Junhua Liu et al. "Causes of interannual variability over the southern hemispheric tropospheric ozone maximum". In: *Atmos. Chem. Phys.* 17.5 (2017), pp. 3279–3299. ISSN: 1680-7324. DOI: [10.5194/acp-17-3279-2017](https://doi.org/10.5194/acp-17-3279-2017). URL: www.atmos-chem-phys.net/17/3279/2017/http://www.atmos-chem-phys.net/17/3279/2017/.
- [108] Yingjun Liu et al. "Isoprene photochemistry over the Amazon rainforest". In: *Proceedings of the National Academy of Sciences* 113.22 (2016), pp. 6125–6130. ISSN: 0027-8424. DOI: [10.1073/pnas.1524136113](https://doi.org/10.1073/pnas.1524136113). URL: <http://www.pnas.org/content/113/22/6125.abstract>.
- [109] Alba Lorente et al. "Structural uncertainty in air mass factor calculation for NO₂ and HCHO satellite retrievals". In: *Atmospheric Measurement Techniques* 2 (2017), pp. 1–35. ISSN: 1867-8610. DOI: [10.5194/amt-10-759-2017](https://doi.org/10.5194/amt-10-759-2017). URL: <https://www.atmos-meas-tech.net/10/759/2017/amt-10-759-2017.html>.
- [110] J. Mao et al. "Insights into hydroxyl measurements and atmospheric oxidation in a California forest". In: *Atmospheric Chemistry and Physics* 12.17 (2012), pp. 8009–8020. ISSN: 16807316. DOI: [10.5194/acp-12-8009-2012](https://doi.org/10.5194/acp-12-8009-2012).
- [111] Jingqiu Mao et al. "Ozone and organic nitrates over the eastern United States: Sensitivity to isoprene chemistry". In: *Journal of Geophysical Research Atmospheres* 118.19 (2013), pp. 11256–11268. ISSN: 21698996. DOI: [10.1002/jgrd.50817](https://doi.org/10.1002/jgrd.50817).
- [112] E A Marais et al. "Isoprene emissions in Africa inferred from OMI observations of formaldehyde columns". In: *Atmospheric Chemistry and Physics* 12.3 (2012), pp. 7475–7520. DOI: [10.5194/acp-12-6219-2012](https://doi.org/10.5194/acp-12-6219-2012). URL: <http://dx.doi.org/10.5194/acp-12-6219-2012>.
- [113] E A Marais et al. "Improved model of isoprene emissions in Africa using Ozone Monitoring Instrument (OMI) satellite observations of formaldehyde: implications for oxidants and particulate matter". In: *Atmospheric Chemistry and Physics* 14.15 (2014), pp. 7693–7703. DOI: [10.5194/acp-14-7693-2014](https://doi.org/10.5194/acp-14-7693-2014). URL: <http://dx.doi.org/10.5194/acp-14-7693-2014>.
- [114] C H Mari et al. "Tracing biomass burning plumes from the Southern Hemisphere during the AMMA 2006 wet season experiment, Atmos". In: *Atmospheric Chemistry and Physics* 8 (2008), pp. 3951–3961. ISSN: 1680-7324. DOI: [10.5194/acpd-7-17339-2007](https://doi.org/10.5194/acpd-7-17339-2007).
- [115] Randall V Martin et al. "Interpretation of TOMS observations of tropical tropospheric ozone with a global model and in situ observations". In: 107 (2002). DOI: [10.1029/2001JD001480](https://doi.org/10.1029/2001JD001480).
- [116] Randall V Martin et al. "Global inventory of nitrogen oxide emissions constrained by space-based observations of NO₂ columns". In: 108.2 (2003), pp. 1–12. DOI: [10.1029/2003JD003453](https://doi.org/10.1029/2003JD003453).
- [117] Margaret R. Marvin et al. "Impact of evolving isoprene mechanisms on simulated formaldehyde: An inter-comparison supported by in situ observations from SENEX". In: *Atmospheric Environment* 164 (2017), pp. 325–336. ISSN: 13522310. DOI: [10.1016/j.atmosenv.2017.05.049](https://doi.org/10.1016/j.atmosenv.2017.05.049). URL: <http://www.sciencedirect.com/science/article/pii/S1352231017303618>.

- [118] Gina M. Mazzuca et al. "Ozone production and its sensitivity to NO_x and VOCs: Results from the DISCOVER-AQ field experiment, Houston 2013". In: *Atmospheric Chemistry and Physics* 16.22 (2016), pp. 14463–14474. ISSN: 16807324. DOI: [10.5194/acp-16-14463-2016](https://doi.org/10.5194/acp-16-14463-2016).
- [119] Palmira Messina et al. "Global biogenic volatile organic compound emissions in the ORCHIDEE and MEGAN models and sensitivity to key parameters". In: *Atmospheric Chemistry and Physics* 16.22 (2016), pp. 14169–14202. ISSN: 16807324. DOI: [10.5194/acp-16-14169-2016](https://doi.org/10.5194/acp-16-14169-2016). URL: <http://www.atmos-chem-phys.net/16/14169/2016/acp-16-14169-2016.pdf>.
- [120] M Mihalikova et al. "Observation of a tropopause fold by MARA VHF wind-profiler radar and ozonesonde at Wasa, Antarctica: comparison with ECMWF analysis and a WRF model simulation". In: *Annales Geophysicae* 30.9 (2012), pp. 1411–1421. DOI: [10.5194/angeo-30-1411-2012](https://doi.org/10.5194/angeo-30-1411-2012). URL: <http://www.ann-geophys.net/30/1411/2012/>.
- [121] C. Miller et al. "Glyoxal retrieval from the Ozone Monitoring Instrument". In: *Atmospheric Measurement Techniques* 7.11 (2014), pp. 3891–3907. ISSN: 1867-8548. DOI: [10.5194/amt-7-3891-2014](https://doi.org/10.5194/amt-7-3891-2014). URL: <http://www.atmos-meas-tech.net/7/3891/2014/>.
- [122] Christopher Chan Miller et al. "Glyoxal yield from isoprene oxidation and relation to formaldehyde: chemical mechanism, constraints from SENEX aircraft observations, and interpretation of OMI satellite data". In: *Atmospheric Chemistry and Physics Discussions* x (2016), pp. 1–25. ISSN: 1680-7375. DOI: [10.5194/acp-2016-1042](https://doi.org/10.5194/acp-2016-1042). URL: <http://www.atmos-chem-phys-discuss.net/acp-2016-1042/>.
- [123] Dylan B Millet et al. "Formaldehyde distribution over North America: Implications for satellite retrievals of formaldehyde columns and isoprene emission". In: *J. Geophys. Res.* 111.D24 (2006). DOI: [10.1029/2005jd006853](https://doi.org/10.1029/2005jd006853). URL: [TODO](http://www.jgr.geophys.res.org/10.1029/2005jd006853).
- [124] Dylan B. Millet et al. "Spatial distribution of isoprene emissions from North America derived from formaldehyde column measurements by the OMI satellite sensor". In: *Journal of Geophysical Research Atmospheres* 113.2 (2008), pp. 1–18. ISSN: 01480227. DOI: [10.1029/2007JD008950](https://doi.org/10.1029/2007JD008950).
- [125] Y Mintz. "The sensitivity of numerically simulated climates to land surface conditions". In: *Land Surface Processes in Atmospheric General Circulation Models* (1982), pp. 109–111.
- [126] P. S. Monks et al. "Tropospheric ozone and its precursors from the urban to the global scale from air quality to short-lived climate forcer". In: *Atmospheric Chemistry and Physics* 15.15 (2015), pp. 8889–8973. ISSN: 1680-7324. DOI: [10.5194/acp-15-8889-2015](https://doi.org/10.5194/acp-15-8889-2015). URL: <http://www.atmos-chem-phys.net/15/8889/2015/>.
- [127] J. F. Müller, J. Peeters, and T. Stavrou. "Fast photolysis of carbonyl nitrates from isoprene". In: *Atmospheric Chemistry and Physics* 14.5 (2014), pp. 2497–2508. ISSN: 16807316. DOI: [10.5194/acp-14-2497-2014](https://doi.org/10.5194/acp-14-2497-2014).

- [128] J.-F. Müller et al. "Global isoprene emissions estimated using MEGAN ECMWF analyses and a detailed canopy environment model". In: *Atmospheric Chemistry and Physics Discussions* 7.6 (2008), pp. 15373–15407. DOI: [10.5194/acpd-7-15373-2007](https://doi.org/10.5194/acpd-7-15373-2007). URL: <http://dx.doi.org/10.5194/acpd-7-15373-2007>.
- [129] Jean-François Müller. "Geographical distribution and seasonal variation of surface emissions and deposition velocities of atmospheric trace gases". In: *Journal of Geophysical Research: Atmospheres* 97.D4 (1992), pp. 3787–3804. ISSN: 2156-2202. DOI: [10.1029/91JD02757](https://doi.org/10.1029/91JD02757). URL: <http://dx.doi.org/10.1029/91JD02757>.
- [130] G Myhre and D Shindell. *Chapter 8: Anthropogenic and Natural Radiative Forcing, in Climate Change 2013: The Physical Science Basis, Working Group 1 Contribution to the Fifth Assessment Report of the Intergovernmental Panel on Climate Change, 2013*. Fifth Assessment Report of the Intergovernmental Panel on Climate Change, 2013., 2013.
- [131] N. Mze et al. "Climatology and comparison of ozone from ENVISAT/GOMOS and SHADOZ/balloon-sonde observations in the southern tropics". In: *Atmospheric Chemistry and Physics* 10.16 (2010), pp. 8025–8035. ISSN: 16807316. DOI: [10.5194/acp-10-8025-2010](https://doi.org/10.5194/acp-10-8025-2010).
- [132] Tran B. Nguyen et al. "Atmospheric fates of Criegee intermediates in the ozonolysis of isoprene". In: *Phys. Chem. Chem. Phys.* 18.15 (2016), pp. 10241–10254. ISSN: 1463-9076. DOI: [10.1039/C6CP00053C](https://doi.org/10.1039/C6CP00053C). URL: <http://xlink.rsc.org/?DOI=C6CP00053C>.
- [133] U. Niinemets et al. "A model of isoprene emission based on energetic requirements for isoprene synthesis and leaf photosynthetic properties for Liquidambar and Quercus". In: *Plant, Cell and Environment* 22.11 (1999), pp. 1319–1335. ISSN: 01407791. DOI: [10.1046/j.1365-3040.1999.00505.x](https://doi.org/10.1046/j.1365-3040.1999.00505.x).
- [134] U. Niinemets et al. "The emission factor of volatile isoprenoids: Stress, acclimation, and developmental responses". In: *Biogeosciences* 7.7 (2010), pp. 2203–2223. ISSN: 17264170. DOI: [10.5194/bg-7-2203-2010](https://doi.org/10.5194/bg-7-2203-2010).
- [135] Narendra Ojha et al. "Secondary ozone peaks in the troposphere over the Himalayas". In: *Atmospheric Chemistry and Physics Discussions* 17.November (2016), pp. 1–25. ISSN: 1680-7375. DOI: [10.5194/acp-2016-908](https://doi.org/10.5194/acp-2016-908). URL: <http://www.atmos-chem-phys-discuss.net/acp-2016-908/>.
- [136] Mark a. Olsen. "A comparison of Northern and Southern Hemisphere cross-tropopause ozone flux". In: *Geophysical Research Letters* 30.7 (2003), p. 1412. ISSN: 0094-8276. DOI: [10.1029/2002GL016538](https://doi.org/10.1029/2002GL016538). URL: <http://doi.wiley.com/10.1029/2002GL016538>.
- [137] J Oltmans et al. "Ozone in the Pacific tropical troposphere from ozonesonde observations". In: *Journal of Geophysical Research* 106.D23 (2001), pp. 32503–32525.
- [138] B.C.a Pak et al. "Measurements of biomass burning influences in the troposphere over southeast Australia during the SAFARI 2000 dry season campaign". In: *Journal of Geophysical Research* 108.13 (2003), pp. 1–10. ISSN: 0148-0227. DOI: [10.1029/2002JD002343](https://doi.org/10.1029/2002JD002343). URL: <http://www.scopus.com/inward/record.url?eid=2-s2.0-0742322536&partnerID=40&md5=cafaeef03b948fb456696583ed3ab9a5>.

- [139] Paul I Palmer. "Mapping isoprene emissions over North America using formaldehyde column observations from space". In: *J. Geophys. Res.* 108.D6 (2003). DOI: [10.1029/2002jd002153](https://doi.org/10.1029/2002jd002153). URL: <http://dx.doi.org/10.1029/2002jd002153>.
- [140] Paul I Palmer et al. "Air mass factor formulation for spectroscopic measurements from satellites' Application to formaldehyde retrievals from the Global Ozone Monitoring Experiment". In: *Journal of Geophysical Research* 106.D13 (2001).
- [141] Paul I Palmer et al. "Quantifying the seasonal and interannual variability of North American isoprene emissions using satellite observations of the formaldehyde column". In: *J. Geophys. Res.* 111 (2006), p. D12315. ISSN: 0148-0227. DOI: [10.1029/2005JD006689](https://doi.org/10.1029/2005JD006689). URL: <http://dx.doi.org/10.1029/2005JD006689>.
- [142] AMIE K. PATCHEN et al. "Direct Kinetics Study of the Product-Forming Channels of the Reaction of Isoprene-Derived Hydroperoxy Radicals with NO". In: *International journal of Chemical Kinetics* 31.5 (2007), pp. 493–499. ISSN: 13000527. DOI: [10.1002/kin](https://doi.org/10.1002/kin). URL: <http://onlinelibrary.wiley.com/doi/10.1002/kin.20248/full>.
- [143] F. Paulot et al. "Isoprene photooxidation: new insights into the production of acids and organic nitrates". In: *Atmospheric Chemistry and Physics* 9.4 (2009), pp. 1479–1501. ISSN: 1680-7324. DOI: [10.5194/acp-9-1479-2009](https://doi.org/10.5194/acp-9-1479-2009).
- [144] Fabien Paulot et al. "Unexpected Epoxide Formation in the". In: *Science* 325.2009 (2009), pp. 730–733. ISSN: 0036-8075. DOI: [10.1126/science.1172910](https://doi.org/10.1126/science.1172910).
- [145] Jozef Peeters and Jean-Francis Muller. "HOx radical regeneration in isoprene oxidation via peroxy radical isomerisations. II: experimental evidence and global impact". In: *Physical Chemistry Chemical Physics* 12.42 (2010), p. 14227. ISSN: 1463-9076. DOI: [10.1039/c0cp00811g](https://doi.org/10.1039/c0cp00811g). URL: <http://pubs.rsc.org/en/content/articlepdf/2010/cp/c0cp00811g>.
- [146] E. Pegoraro et al. "Effect of drought on isoprene emission rates from leaves of *Quercus virginiana* Mill." In: *Atmospheric Environment* 38.36 (2004), pp. 6149–6156. ISSN: 13522310. DOI: [10.1016/j.atmosenv.2004.07.028](https://doi.org/10.1016/j.atmosenv.2004.07.028). URL: <http://linkinghub.elsevier.com/retrieve/pii/S1352231004007198>.
- [147] William H Press et al. *Numerical Recipes in C (2Nd Ed.): The Art of Scientific Computing*. New York, NY, USA: Cambridge University Press, 1992. ISBN: 0-521-43108-5.
- [148] J. D. Price and G. Vaughan. "The potential for stratosphere-troposphere exchange in cut-off-low systems". In: *Quarterly Journal of the Royal Meteorological Society* 119.510 (1993), pp. 343–365. DOI: [10.1002/qj.49711951007](https://doi.org/10.1002/qj.49711951007). URL: <http://onlinelibrary.wiley.com/doi/10.1002/qj.49711951007/abstract>.
- [149] P. Reutter et al. "Stratosphere-troposphere exchange (STE) in the vicinity of North Atlantic cyclones". In: *Atmospheric Chemistry and Physics* 15.19 (2015), pp. 10939–10953. ISSN: 16807324. DOI: [10.5194/acp-15-10939-2015](https://doi.org/10.5194/acp-15-10939-2015).
- [150] Michele Rienecker. "File Specification for GEOS-5 DAS Gridded Output". In: (2007), pp. 1–54. URL: https://gmao.gsfc.nasa.gov/products/documents/GEOS-5.1.0_File_Specification.pdf.

- [151] Geert Jan Roelofs and Jos Lelieveld. *Model study of the influence of cross-tropopause O₃ transports on tropospheric O₃ levels*. 1997. DOI: [10.1034/j.1600-0889.49.issue1.3.x](https://doi.org/10.1034/j.1600-0889.49.issue1.3.x).
- [152] A W Rollins et al. "Isoprene oxidation by nitrate radical: alkyl nitrate and secondary organic aerosol yields". In: *Atmos. Chem. Phys. Atmospheric Chemistry and Physics* 9 (2009), pp. 6685–6703. URL: www.atmos-chem-phys.net/9/6685/2009/.
- [153] P. R. Rowntree and J. A. Bolton. "Simulation of the atmospheric response to soil moisture anomalies over Europe". In: *Quarterly Journal of the Royal Meteorological Society* 109.461 (1983), pp. 501–526. ISSN: 00359009. DOI: [10.1002/qj.49710946105](https://doi.org/10.1002/qj.49710946105). URL: <http://doi.wiley.com/10.1002/qj.49710946105>.
- [154] R Sander et al. "Technical note: The new comprehensive atmospheric chemistry module MECCA". In: *Atmospheric Chemistry and Physics* 5.2 (2005), pp. 445–450. ISSN: 1680-7324. DOI: [10.5194/acp-5-445-2005](https://doi.org/10.5194/acp-5-445-2005). URL: <http://www.atmos-chem-phys.net/5/445/2005/>.
- [155] A Sandu and R Sander. "Technical note: Simulating chemical systems in Fortran90 and Matlab with the Kinetic PreProcessor KPP-2.1". In: *Atmospheric Chemistry and Physics* 6.1 (2006), pp. 187–195. DOI: [10.5194/acp-6-187-2006](https://doi.org/10.5194/acp-6-187-2006). URL: <http://www.atmos-chem-phys.net/6/187/2006/>.
- [156] V. M. Erik Schenkeveld et al. "In-flight performance of the Ozone Monitoring Instrument". In: *Atmospheric Measurement Techniques* 10.5 (2017), pp. 1957–1986. ISSN: 1867-8548. DOI: [10.5194/amt-10-1957-2017](https://doi.org/10.5194/amt-10-1957-2017). URL: <http://www.atmos-meas-tech-discuss.net/amt-2016-420/> <https://www.atmos-meas-tech.net/10/1957/2017/>.
- [157] Stefan F. Schreier et al. "Estimates of free-Tropospheric NO₂ and HCHO mixing ratios derived from high-Altitude mountain MAX-DOAS observations at mid-latitudes and in the tropics". In: *Atmospheric Chemistry and Physics* 16.5 (2016). ISSN: 16807324. DOI: [10.5194/acp-16-2803-2016](https://doi.org/10.5194/acp-16-2803-2016).
- [158] N E Selin et al. "Global health and economic impacts of future ozone pollution". In: *Environmental Research Letters* 4.4 (2009), p. 044014. ISSN: 1748-9326. DOI: [10.1088/1748-9326/4/4/044014](https://doi.org/10.1088/1748-9326/4/4/044014).
- [159] Changsub Shim et al. "Constraining global isoprene emissions with Global Ozone Monitoring Experiment (GOME) formaldehyde column measurements". In: *Journal of Geophysical Research Atmospheres* 110.24 (2005), pp. 1–14. ISSN: 01480227. DOI: [10.1029/2004JD005629](https://doi.org/10.1029/2004JD005629).
- [160] Raquel A Silva et al. "Global premature mortality due to anthropogenic outdoor air pollution and the contribution of past climate change". In: *Environ. Res. Lett.* 8.3 (2013), p. 34005. DOI: [10.1088/1748-9326/8/3/034005](https://doi.org/10.1088/1748-9326/8/3/034005). URL: <http://dx.doi.org/10.1088/1748-9326/8/3/034005>.
- [161] K. Sindelarova et al. "Global data set of biogenic VOC emissions calculated by the MEGAN model over the last 30 years". In: *Atmospheric Chemistry and Physics* 14.17 (2014), pp. 9317–9341. ISSN: 16807324. DOI: [10.5194/acp-14-9317-2014](https://doi.org/10.5194/acp-14-9317-2014). arXiv: [arXiv:1011.1669v3](https://arxiv.org/abs/1011.1669v3).

- [162] Parikhith Sinha et al. "Transport of biomass burning emissions from southern Africa". In: *Journal of Geophysical Research* 109 (2004), p. D20204. ISSN: 01480227. DOI: [10.1029/2004JD005044](https://doi.org/10.1029/2004JD005044).
- [163] B Škerlak, M Sprenger, and H Wernli. "A global climatology of stratosphere-troposphere exchange using the ERA-Interim data set from 1979 to 2011". In: *Atmospheric Chemistry and Physics* 14.2 (2014), pp. 913–937. DOI: [10.5194/acp-14-913-2014](https://doi.org/10.5194/acp-14-913-2014). URL: <http://www.atmos-chem-phys.net/14/913/2014/>.
- [164] Bojan Škerlak et al. "Tropopause folds in ERA-Interim: Global climatology and relation to extreme weather events". In: *Journal of Geophysical Research* 120.10 (2015), pp. 4860–4877. ISSN: 21698996. DOI: [10.1002/2014JD022787](https://doi.org/10.1002/2014JD022787).
- [165] Herman G J Smit et al. "Assessment of the performance of ECC-ozonesondes under quasi-flight conditions in the environmental simulation chamber: Insights from the Juelich Ozone Sonde Intercomparison Experiment (JOSIE)". In: *Journal of Geophysical Research* 112.19 (2007), pp. 1–18. ISSN: 01480227. DOI: [10.1029/2006JD007308](https://doi.org/10.1029/2006JD007308).
- [166] SPEI Drought Index. URL: <http://spei.csic.es/home.html> (visited on 12/19/2017).
- [167] Michael Sprenger, Mischa Croci Maspoli, and Heini Wernli. "Tropopause folds and cross-tropopause exchange: A global investigation based upon ECMWF analyses for the time period March 2000 to February 2001". In: *Journal of Geophysical Research* 108.D12 (2003). ISSN: 2156-2202. DOI: [10.1029/2002JD002587](https://doi.org/10.1029/2002JD002587). URL: <http://dx.doi.org/10.1029/2002JD002587>.
- [168] R. J D Spurr. "Simultaneous derivation of intensities and weighting functions in a general pseudo-spherical discrete ordinate radiative transfer treatment". In: *Journal of Quantitative Spectroscopy and Radiative Transfer* 75.2 (2002), pp. 129–175. ISSN: 00224073. DOI: [10.1016/S0022-4073\(01\)00245-X](https://doi.org/10.1016/S0022-4073(01)00245-X).
- [169] T Stavrakou et al. "Evaluating the performance of pyrogenic and biogenic emission inventories against one decade of space-based formaldehyde columns". In: *Atmospheric Chemistry and Physics* 9.3 (2009), pp. 1037–1060. DOI: [10.5194/acp-9-1037-2009](https://doi.org/10.5194/acp-9-1037-2009). URL: <http://dx.doi.org/10.5194/acp-9-1037-2009>.
- [170] T. Stavrakou et al. "Isoprene emissions over Asia 1979-2012: Impact of climate and land-use changes". In: *Atmospheric Chemistry and Physics* 14.9 (2014). ISSN: 16807324. DOI: [10.5194/acp-14-4587-2014](https://doi.org/10.5194/acp-14-4587-2014).
- [171] T. Stavrakou et al. "How consistent are top-down hydrocarbon emissions based on formaldehyde observations from GOME-2 and OMI?" English. In: *Atmospheric Chemistry and Physics* 15.20 (2015), pp. 11861–11884. ISSN: 1680-7324. DOI: [10.5194/acp-15-11861-2015](https://doi.org/10.5194/acp-15-11861-2015). URL: <http://www.atmos-chem-phys.net/15/11861/2015/acp-15-11861-2015.html>.
- [172] D S Stevenson et al. "Multimodel ensemble simulations of present-day and near-future tropospheric ozone". In: *Journal of Geophysical Research* 111.D8 (2006). DOI: [10.1029/2005jd006338](https://doi.org/10.1029/2005jd006338). URL: <http://dx.doi.org/10.1029/2005JD006338>.

- [173] D. S. Stevenson et al. "Tropospheric ozone changes, radiative forcing and attribution to emissions in the Atmospheric Chemistry and Climate Model Intercomparison Project (ACCMIP)". In: *Atmospheric Chemistry and Physics* 13.6 (2013), pp. 3063–3085. ISSN: 16807316. DOI: [10.5194/acp-13-3063-2013](https://doi.org/10.5194/acp-13-3063-2013).
- [174] T.F. Stocker et al. *IPCC, 2013: Climate Change 2013: The Physical Science Basis. Contribution of Working Group I to the Fifth Assessment Report of the Intergovernmental Panel on Climate Change*. Tech. rep. Cambridge University Press, Cambridge, United Kingdom and New York, NY, USA. DOI: [10.1017/CB09781107415324](https://doi.org/10.1017/CB09781107415324).
- [175] Andreas Stohl et al. "A new perspective of stratosphere-troposphere exchange". In: *Bulletin of the American Meteorological Society* 84.11 (2003), pp. 1565–1573+1473. ISSN: 00030007. DOI: [10.1175/BAMS-84-11-1565](https://doi.org/10.1175/BAMS-84-11-1565).
- [176] H. Struthers et al. "Past and future simulations of NO₂ from a coupled chemistry-climate model in comparison with observations". In: *Atmospheric Chemistry and Physics* 4.8 (2004), pp. 2227–2239. ISSN: 1680-7324. DOI: [10.5194/acp-4-2227-2004](https://doi.org/10.5194/acp-4-2227-2004). URL: <http://www.atmos-chem-phys.net/4/2227/2004/>.
- [177] Q. Tang and M. J. Prather. "Correlating tropospheric column ozone with tropopause folds: The Aura-OMI satellite data". In: *Atmospheric Chemistry and Physics* 10.19 (2010), pp. 9681–9688. ISSN: 16807316. DOI: [10.5194/acp-10-9681-2010](https://doi.org/10.5194/acp-10-9681-2010).
- [178] Q. Tang and M. J. Prather. "Five blind men and the elephant: What can the NASA Aura ozone measurements tell us about stratosphere-troposphere exchange?" In: *Atmospheric Chemistry and Physics* 12.5 (2012), pp. 2357–2380. ISSN: 16807316. DOI: [10.5194/acp-12-2357-2012](https://doi.org/10.5194/acp-12-2357-2012). URL: <http://dx.doi.org/10.5194/acpd-11-26897-2011>.
- [179] Yukio Terao et al. "Contribution of stratospheric ozone to the interannual variability of tropospheric ozone in the northern extratropics". In: *Journal of Geophysical Research* 113.D18 (2008). DOI: [10.1029/2008jd009854](https://doi.org/10.1029/2008jd009854). URL: <http://dx.doi.org/10.1029/2008jd009854>.
- [180] Joao Teixeira. *AIRS/Aqua L3 Daily Standard Physical Retrieval (AIRS-only) 1 degree x 1 degree V006: Accessed 2/Dec/2015*. 2013. DOI: [doi : 10.5067 / AQUA / AIRS / DATA303](https://doi.org/10.5067/AQUA/AIRS/DATA303).
- [181] W Thomas et al. "Detection of biomass burning combustion products in South-east Asia from backscatter data taken by the GOME spectrometer". In: *Geophysical Research Letters* 25.9 (1998), pp. 1317–1320. DOI: [10.1029/98GL01087](https://doi.org/10.1029/98GL01087). URL: <http://onlinelibrary.wiley.com/doi/10.1029/98GL01087/epdf>.
- [182] A. M. Thompson et al. "Tropospheric ozone increases over the southern Africa region: Bellwether for rapid growth in Southern Hemisphere pollution?" In: *Atmospheric Chemistry and Physics* 14.18 (2014), pp. 9855–9869. ISSN: 16807324. DOI: [10.5194/acp-14-9855-2014](https://doi.org/10.5194/acp-14-9855-2014).
- [183] Yoshihiro Tomikawa, Yashiro Nishimura, and Takashi Yamanouchi. "Characteristics of Tropopause and Tropopause Inversion Layer in the Polar Region". In: *SOLA* 5 (2009), pp. 141–144. DOI: [10.2151/sola.2009-036](https://doi.org/10.2151/sola.2009-036). URL: <http://dx.doi.org/10.2151/sola.2009-036>.

- [184] Katherine R Travis et al. "Why do models overestimate surface ozone in the Southeast United States?" In: *Atmos. Chem. Phys* 16 (2016), pp. 13561–13577. DOI: [10.5194/acp-16-13561-2016](https://doi.org/10.5194/acp-16-13561-2016). URL: www.atmos-chem-phys.net/16/13561/2016/.
- [185] T. Trickl et al. "How stratospheric are deep stratospheric intrusions?" In: *Atmospheric Chemistry and Physics* 14.18 (2014), pp. 9941–9961. ISSN: 16807324. DOI: [10.5194/acp-14-9941-2014](https://doi.org/10.5194/acp-14-9941-2014).
- [186] Evangelos Tyrlis et al. "On the linkage between the Asian summer monsoon and tropopause fold activity over the eastern Mediterranean and the Middle East". In: *Journal of Geophysical Research* 119.6 (2014), pp. 3202–3221. ISSN: 2169897X. DOI: [10.1002/2013JD021113](https://doi.org/10.1002/2013JD021113). URL: <http://doi.wiley.com/10.1002/2013JD021113>.
- [187] R J VanDerA et al. "Trends seasonal variability and dominant NO_x source derived from a ten year record of NO₂ measured from space". In: *J. Geophys. Res.* 113.D4 (2008). DOI: [10.1029/2007jd009021](https://doi.org/10.1029/2007jd009021). URL: <http://dx.doi.org/10.1029/2007jd009021>.
- [188] A Vasilkov et al. "Accounting for the effects of surface BRDF on satellite cloud and trace-gas retrievals: a new approach based on geometry-dependent Lambertian equivalent reflectivity applied to OMI algorithms". In: *Atmospheric Measurement Techniques* 10.1 (2017), pp. 333–349. DOI: [10.5194/amt-10-333-2017](https://doi.org/10.5194/amt-10-333-2017). URL: <http://www.atmos-meas-tech.net/10/333/2017/>.
- [189] G. Vaughan, J. D. Price, and A. Howells. "Transport into the troposphere in a tropopause fold". In: *Quarterly Journal of the Royal Meteorological Society* 120.518 (1993), pp. 1085–1103. ISSN: 00359009. DOI: [10.1002/qj.49712051814](https://doi.org/10.1002/qj.49712051814).
- [190] C. Vigouroux et al. "Ground-based FTIR and MAX-DOAS observations of formaldehyde at Réunion Island and comparisons with satellite and model data". In: *Atmospheric Chemistry and Physics Discussions* 9 (2009), pp. 15891–15957. ISSN: 1680-7316. DOI: [10.5194/acpd-9-15891-2009](https://doi.org/10.5194/acpd-9-15891-2009).
- [191] V Wagner. "Are CH₂O measurements in the marine boundary layer suitable for testing the current understanding of CH₄ photooxidation?: A model study". In: *Journal of Geophysical Research* 107.D3 (2002), p. 4029. ISSN: 0148-0227. DOI: [10.1029/2001JD000722](https://doi.org/10.1029/2001JD000722). URL: <http://doi.wiley.com/10.1029/2001JD000722>.
- [192] Yuxuan Wang et al. "Adverse effects of increasing drought on air quality via natural processes". In: *Atmos. Chem. Phys* 17.194 (2017), pp. 12827–12843. DOI: [10.5194/acp-17-12827-2017](https://doi.org/10.5194/acp-17-12827-2017). URL: <https://www.atmos-chem-phys.net/17/12827/2017/acp-17-12827-2017.pdf>.
- [193] Wiel M F Wauben, J Paul F Fortuin, and Peter F J Van Velthoven. "Comparison of modeled ozone distributions observations". In: *Journal of Geophysical Research* 103 (1998), pp. 3511–3530.
- [194] Wikipedia. *Solar zenith angle*. 2016. DOI: [10.1016/B978-012369407-2/50005-X](https://doi.org/10.1016/B978-012369407-2/50005-X). URL: <http://sacs.aeronomie.be/info/sza.php>.
- [195] Oliver Wild and Michael J. Prather. "Global tropospheric ozone modeling: Quantifying errors due to grid resolution". In: *Journal of Geophysical Research Atmospheres* 111.11 (2006), pp. 1–14. ISSN: 01480227. DOI: [10.1029/2005JD006605](https://doi.org/10.1029/2005JD006605).

- [196] Anthony J Winters et al. "Emissions of isoprene, monoterpene and short-chained carbonyl compounds from Eucalyptus spp. in southern Australia". In: *Atmospheric Environment* 43.19 (2009), pp. 3035–3043. ISSN: 13522310. DOI: [10.1016/j.atmosenv.2009.03.026](https://doi.org/10.1016/j.atmosenv.2009.03.026).
- [197] Volkmar Wirth. "Diabatic heating in an axisymmetric cut-off cyclone and related stratosphere-troposphere exchange". In: *Quarterly Journal of the Royal Meteorological Society* 121.521 (1995), pp. 127–147. ISSN: 00359009. DOI: [10.1002/qj.49712152107](https://doi.org/10.1002/qj.49712152107). URL: <http://doi.wiley.com/10.1002/qj.49712152107>.
- [198] World Meteorological Organization WMO. "Meteorology A Three-Dimensional Science". In: *Geneva, Second Session of the Commission for Aerology* 4 (1957), pp. 134–138.
- [199] G M Wolfe et al. "Formaldehyde production from isoprene oxidation". In: *Atmospheric Chemistry and Physics* 16.x (2016), pp. 2597–2610. DOI: [10.5194/acp-16-2597-2016](https://doi.org/10.5194/acp-16-2597-2016). URL: www.atmos-chem-phys.net/16/2597/2016/.
- [200] P. J. Young et al. "Preindustrial to present-day changes in tropospheric hydroxyl radical and methane lifetime from the Atmospheric Chemistry and Climate Model Intercomparison Project (ACCMIP)". In: *Atmospheric Chemistry and Physics* 13.10 (2013), pp. 5277–5298. ISSN: 16807316. DOI: [10.5194/acp-13-5277-2013](https://doi.org/10.5194/acp-13-5277-2013).
- [201] X. Yue, N. Unger, and Y. Zheng. "Distinguishing the drivers of trends in land carbon fluxes and plant volatile emissions over the past 3 decades". In: *Atmospheric Chemistry and Physics* 15.20 (2015), pp. 11931–11948. ISSN: 16807324. DOI: [10.5194/acp-15-11931-2015](https://doi.org/10.5194/acp-15-11931-2015).
- [202] Xu Yue et al. "Ozone and haze pollution weakens net primary productivity in China". In: *Atmospheric Chemistry and Physics* 17.9 (2017), pp. 6073–6089. ISSN: 1680-7324. DOI: [10.5194/acp-17-6073-2017](https://doi.org/10.5194/acp-17-6073-2017). URL: <https://www.atmos-chem-phys.net/17/6073/2017/>.
- [203] P. Zanis et al. "Summertime free-tropospheric ozone pool over the eastern Mediterranean/middle east". In: *Atmospheric Chemistry and Physics* 14.1 (2014), pp. 115–132. ISSN: 16807316. DOI: [10.5194/acp-14-115-2014](https://doi.org/10.5194/acp-14-115-2014).
- [204] G. Zeng et al. "Multi-model simulation of CO and HCHO in the Southern Hemisphere: comparison with observations and impact of biogenic emissions". In: *Atmospheric Chemistry and Physics* 15.13 (2015), pp. 7217–7245. ISSN: 1680-7324. DOI: [10.5194/acp-15-7217-2015](https://doi.org/10.5194/acp-15-7217-2015). URL: <http://www.atmos-chem-phys.net/15/7217/2015/>.
- [205] L Zhang et al. "Sources contributing to background surface ozone in the US Intermountain West". In: *Atmospheric Chemistry and Physics* 14.11 (2014), pp. 5295–5309. DOI: [10.5194/acp-14-5295-2014](https://doi.org/10.5194/acp-14-5295-2014). URL: <http://dx.doi.org/10.5194/acp-14-5295-2014>.
- [206] Yang Zhang et al. "Impact of gas-phase mechanisms on Weather Research Forecasting Model with Chemistry (WRF/Chem) predictions: Mechanism implementation and comparative evaluation". In: *Journal of Geophysical Research: Atmospheres* 117.D1 (2012), n/a–n/a. DOI: [10.1029/2011JD015775](https://doi.org/10.1029/2011JD015775). URL: <http://doi.wiley.com/10.1029/2011JD015775>.

- [207] Lei Zhu et al. "Variability of HCHO over the Southeastern United States observed from space : Implications for VOC emissions". In: vol. 1. 2013.
- [208] Lei Zhu et al. "Anthropogenic emissions of highly reactive volatile organic compounds in eastern Texas inferred from oversampling of satellite (OMI) measurements of HCHO columns". In: *Environmental Research Letters* 9.11 (2014), p. 114004. ISSN: 1748-9326. DOI: [10 . 1088 / 1748 - 9326 / 9 / 11 / 114004](https://doi.org/10.1088/1748-9326/9/11/114004). URL: <http://stacks.iop.org/1748-9326/9/i=11/a=114004?key=crossref.3d2869ee02fd4f0792f831ac8cbe117>.
- [209] Lei Zhu et al. "Observing atmospheric formaldehyde (HCHO) from space: validation and intercomparison of six retrievals from four satellites (OMI, GOME2A, GOME2B, OMPS) with SEAC4RS aircraft observations over the Southeast US". In: *Atmospheric Chemistry and Physics* 0 (2016), pp. 1–24. ISSN: 1680-7375. DOI: [10.5194/acp-2016-162](https://doi.org/10.5194/acp-2016-162). URL: <http://www.atmos-chem-phys.net/16/13477/2016/acp-16-13477-2016.pdf>.